IN-34
7618

NASA Technical Memorandum 102616

p.51

Addition of Equilibrium Air to an Upwind Navier-Stokes Code and Other First Steps Toward a More Generalized Flow Solver

Bruce S. Rosen

March 1991

NASA
National Aeronautics and Space Administration

Langley Research Center
Hampton, Virginia 23665

Addition of Equilibrium Air to an Upwind Navier-Stokes Code and Other First Steps toward a More Generalized Flow Solver*

Bruce S. Rosen†
Grumman Aircraft Systems Division
Bethpage, NY 11714

ABSTRACT

An upwind 3-D finite volume Navier-Stokes code is modified to facilitate modeling of complex geometries and flow fields presented by proposed National Aero-Space Plane concepts. Code enhancements include an equilibrium air model, a generalized equilibrium gas model, and several schemes to simplify treatment of complex geometric configurations. The code is also restructured for inclusion of an arbitrary number of independent and dependent variables. This latter capability is intended for eventual use to incorporate nonequilibrium/chemistry gas models, more sophisticated turbulence and transition models, or other physical phenomena which will require inclusion of additional variables and/or governing equations. Comparisons of computed results with experimental data and with results obtained using other methods are presented for code validation purposes. Good correlation is obtained for all of the test cases considered, indicating the success of the current effort. This work was conducted at the NASA Langley Research Center, during participation in the NASA/Industry Fellowship Program for the National Aero-Space Plane.

*This work was conducted at the NASA Langley Research Center, during participation in the NASA/Industry Fellowship Program for the National Aero-Space Plane

†Engineering Specialist

INTRODUCTION

The National Aero-Space Plane (NASP) program has highlighted the need for development of advanced computational fluid dynamics methodology. The success of the program, unlike that for any previous aircraft, depends upon the availability of the state-of-the-art in flow simulation and prediction. Advances in flow discretization techniques, solution algorithms, equilibrium and nonequilibrium/chemistry gas models, and turbulence and transition models must be incorporated into methodology capable of treating the complex geometries and flow fields presented by proposed NASP concepts.

The NASA/Industry Fellowship Program provided this author with an opportunity to assist in the development of one such method. The basic CFL3D code, an advanced thin-layer Navier-Stokes flow solver which is relatively easy to use and which features the flexibility required to treat complex flows, was modified during this effort to incorporate equilibrium air and generalized equilibrium gas models, and to further enhance its geometric modeling capabilities. At the same time, the code was restructured to facilitate future computations incorporating an arbitrary number of independent and dependent variables. This latter capability is intended for eventual use to incorporate nonequilibrium/chemistry gas models, more sophisticated turbulence and transition models, or other physical phenomena which will require inclusion of additional variables and/or governing equations.

NOMENCLATURE

a	speed of sound
e	internal energy per unit mass
L	reference length
M	Mach number
p	pressure
Pr	Prandtl number
Re	Reynolds number
T	temperature
u,v,w	Cartesian velocity components
x,y,z	Cartesian spatial coordinates

y^+	wall unit, $\Delta y \cdot (\rho_w \, \omega_w \,/\, \mu_w)^{1/2}$
γ	specific heat ratio
$\tilde{\gamma}$	"equivalent" specific heat ratio, $1 + p \,/\, \rho\, e$
Γ	"equivalent" specific heat ratio, $a^2 \rho \,/\, p$
ρ	mass per unit volume (density)
κ	thermal conductivity
μ	viscosity
ω	vorticity

Subscripts

∞	freestream
w	wall

DESCRIPTION OF METHOD

The computer program to be described is derived from the April 1988 release of CFL3D (Version 1.0), a method which is well documented in the open literature [1,2,3,4]. A brief outline of CFL3D methodology is given below, followed by a discussion of enhancements and features incorporated in the present code.

Overview of Basic CFL3D Methodology

The governing flow equations are the three-dimensional, time-dependent, conservation law form of the compressible Euler or thin-layer Reynolds-averaged Navier-Stokes equations, expressed in generalized coordinates. An upwind-biased approach with up to third order accuracy is used to evaluate the inviscid fluxes at the cell interfaces, as described below. A spatially-split, three-factor approximate factorization algorithm and Euler implicit time integration/linearization is used to advance the solution (cell-averaged flow properties) in time [5].

Inviscid flux interface values are obtained using a MUSCL interpolation scheme [6], coupled to either the flux difference splitting (FDS) scheme of Roe [7,8] or the flux vector splitting (FVS) scheme of Van Leer [5,9]. Flux splittings are based on a one-dimensional Riemann problem, and are subsequently modified to treat multi-dimensional flows. Overall, these approaches provide an upwind-biasing in the flux interface evaluation. They also introduce an amount of dissipation which is consistent with the discretization of the governing flow equations, and which is required to stabilize the solution procedure. The so-called smooth and min-mod flux gradient limiters are optionally employed, to minimize the adverse effects of large flow gradients and discontinuities (such as shock waves).

At each time step, the FDS/FVS approaches lead to a series of 5-by-5 block tridiagonal matrix inversions, for each of the spatial directions. Additional approximations may also be made in the FDS scheme so as to diagonalize the solution matrices [3]. This leads to a series of scalar tridiagonal matrix inversions, and an attendant reduction in execution time.

Viscous and heat flux interface values are obtained using central finite-difference formulae. The laminar thin-layer Navier-Stokes terms may be included in all three directions. A Baldwin-Lomax algebraic turbulence model [10] is also employed. The effects of turbulence may be included in one direction, or in two directions via a distance-weighted two-wall corner model for the turbulent eddy viscosity.

A zonal grid structure facilitates modeling of complex geometries and/or flow fields. Explicit treatment of grid boundaries further simplifies this task, since boundary condition subroutines are easily modified for specific or unusual cases. Provisions are included for treatment of blocked grids, longitudinally-patched grids [11], and dynamic moving grids. A variety of cell-center or cell-interface type boundary conditions may also be specified at grid boundaries ... freestream flow, extrapolation from the interior (supersonic outflow), subsonic characteristic inflow/outflow (based on one-dimensional Riemann invariants [12]), inviscid wall (flow tangency), viscous wall (adiabatic or fixed wall temperature), and an assortment of symmetry/periodicity/singular-axis/wake-continuation type boundary conditions.

Several schemes are available to reduce overall execution time, particularly for computing steady flows. Local-time-stepping and multigrid [12,13,14] techniques accelerate code convergence. Mesh sequencing is a technique whereby solutions obtained on coarser grids are used to initialize flow field data on successively finer grids, until finally a solution is obtained on the desired input grid. Mesh embedding is a technique whereby enhanced solution accuracy is obtained by locating even finer grids in particular regions of interest. Both mesh sequencing and mesh embedding reduce the computational effort expended to achieve a given level of solution accuracy, and their use is facilitated by automated grid generation and flow field interpolation routines.

In February 1989, while the present code was still under development, an updated version of CFL3D (Version 1.1) became available. The enhanced capabilities of the updated version of CFL3D were subsequently incorporated in the present code, including an improved treatment for longitudinally-patched grids [15], more generalized boundary conditions, and mesh sequencing for two-dimensional flows. The only CFL3D enhancement not found in the present code is an alternate two-factor approximate factorization algorithm [12].

Equilibrium Air and Generalized Equilibrium Gas Models

The methodology described above assumes a perfect gas model for the thermodynamic and transport properties of the fluid. Versions 1.0 and 1.1 of CFL3D further assume air to be the working fluid. These restrictions do not apply to the present code, which features more general equilibrium gas capabilities.

The flux-splitting schemes of Roe and Van Leer are extended in the present code to treat real gases, using techniques developed by Grossman and Walters [16]. The perfect gas relationships are replaced by equilibrium gas relationships, usually in the form of curve fits. The specific heat ratio γ employed in the flux-splitting schemes is then replaced by the "equivalent" values $\tilde{\gamma} = 1 + p / \rho e$ and $\Gamma = a^2 \rho / p$.

Two equilibrium gas models for thermodynamic properties (ρ, p, e, a and T) are incorporated into the present code. The first, due to Srinivasan and Tannehill [17], consists of curve fits for equilibrium air, and executes in scalar mode. The second, due to Liu and Vinokur [18], is a generalized equilibrium gas model, uses bicubic spline interpolation (based on an auxiliary interpolation coefficient data file), and executes in vector mode. An interpolation coefficient file for equilibrium air obtained from Liu was augmented by this author in order to use the approach at lower temperatures normally considered to be in the perfect gas regime.

The equilibrium gas model for transport properties (μ, κ, and Pr) is the equilibrium air curve fits due to Srinivasan and Tannehill [19]. Versions which execute in vector mode were developed by this author, after discovering that more execution time was used for computing transport properties than for computing thermodynamic properties.

The Liu and Vinokur thermodynamic property model is not restricted to equilibrium air, since auxiliary interpolation coefficient data files for other equilibrium gases could be constructed. A similar approach for the transport properties is hopefully under development, and when available can be incorporated into the present code as well.

Relative to perfect gas computations, the original (scalar) Srinivasan and Tannehill thermodynamic and transport property gas models result in roughly a 125% increase in execution time. Using the vectorized Srinivasan and Tannehill transport property model results in only about a 50% increase in execution time, while using the vectorized Srinivasan and Tannehill transport property model and the vectorized Liu and Vinokur thermodynamic property model results in only about a 20% increase in execution time. Of course, these numbers are approximate, and reflect average values obtained for a variety of test cases.

First Steps towards a More Generalized Flow Solver

In conjunction with the equilibrium gas flux-splitting capability, the present code was enhanced so as to permit an arbitrary number of independent and dependent variables to be stored in the q-vector.

The basic CFL3D code stores only the five independent variables ρ, u, v, w, and p in the q-vector. In the present code, an arbitrary number of independent variables (i.e., the number of conserved variables or governing equations), *lqcv*, and an arbitrary number of dependent variables (e.g., $\tilde{\gamma}$ and Γ), *lqdv*, may be stored in the q-vector. The values of *lqcv* and *lqdv* need be set only once, in a parameter statement in the main program. These values, and the total number of variables in the q-vector, $lqt = lqcv + lqdv$, are subsequently passed to the required subroutines as arguments and/or through common blocks, for appropriate dimensioning of arrays and indexing of do loops.

This coding structure is a first step towards a more generalized flow solver which might incorporate nonequilibrium/chemistry gas effects, more sophisticated turbulence and transition modeling, or other physical phenomena which will require inclusion of additional variables and/or governing equations. Additional work will be required before this goal is achieved. For example, matrix inversion logic is currently fixed to treat 5 governing equations, and increasing the value of lqt may result in overlap or overflow of flux routine scratch arrays. Nevertheless, the majority of the present code should not require further modification in order to incorporate more generalized flow models.

Other Code Enhancements

Two important features of the present code were developed to enhance user friendliness. First, the path and name of all auxiliary data files (currently as many as 11) are specified via the standard unit 5 input data, rather than in the FORTRAN coding itself, to avoid code modification and recompilation. Second, user specified scale factors for length, mass, and temperature permit the use of arbitrary dimensions (e.g., metric or English) for the input and output data.

Other features of the present code offer enhanced capabilities. Most significant of these is a very generalized grid blocking boundary condition capability (developed by George Switzer, Analytical Services and Materials, Inc.). Also noteworthy is a "jagged" boundary condition algorithm (developed by Mark Eppard, Analytical Services and Materials, Inc.) which permits treatment of surface edges that are skewed with respect to, or cut across, grid lines. A new flux interface averaging procedure, developed at NASA Langley, may enhance convergence for cold wall cases. Since the jagged boundary condition and flux interface averaging capabilities are not yet fully generalized, they have been commented out in the FORTRAN coding (lines start with the characters "cbsr"), and should be activated only by knowledgeable users.

RESULTS

Results computed for several test cases are presented in order to evaluate the present code's capabilities. For each test case, calculations are compared to results obtained using other methods, or to experimental data, and previous comparisons by other investigators are cited.

Computations were obtained using the perfect gas model, the Srinivasan and Tannehill equilibrium air model, and the Liu and Vinokur generalized equilibrium gas model with the augmented auxiliary interpolation coefficient data file for equilibrium air. Since the two equilibrium air models gave essentially identical results for all of the test cases, only those obtained with the Liu and Vinokur model are presented herein.

Unless otherwise noted, all results were computed using FDS, third order upwind-biased spatial accuracy, min-mod flux limiter, and the 5-by-5 block tridiagonal matrix inversion algorithm. The majority of the computations were made for laminar flow, and included thin-layer terms in the *k*-direction (normal to the body surface) only. A fixed wall temperature was specified for use in all viscous wall boundary conditions. Local time stepping was used to accelerate convergence to steady state.

Supersonic Laminar Flat Plate Boundary Layer

The first test case consists of supersonic laminar flow over a flat plate (this is also one of the test cases studied in [20]). The flow conditions are:

$$
\begin{aligned}
M_\infty &= 2.0 \\
Re_\infty/L &= 1.65\cdot 10^6 / m \\
T_\infty &= 221.6\ ^\circ K \\
T_W &= 221.6\ ^\circ K
\end{aligned}
$$

A grid consisting of 51 grid points in the streamwise direction and 100 grid points normal to the surface was employed. Average grid spacing normal to the surface was $0.43 \cdot 10^{-4}\ m$, producing an average y^+ of 1.33. The residual was reduced approximately 4.5 orders of magnitude over 4000 time steps. NASA Cray-YMP (Reynolds) execution times required for the perfect gas, Srinivasan and Tannehill, and Liu and Vinokur gas models were $4.5 \cdot 10^{-5}$, $7.2 \cdot 10^{-5}$, and $5.4 \cdot 10^{-5}$ cpu-seconds per mesh-cell-point per time-step-iteration, respectively.

Computed supersonic laminar flat plate boundary layer results are compared to predictions made using a conventional boundary layer calculation [21] (boundary layer calculations supplied by Douglas Dilley, Analytical Services and Materials, Inc.). Velocity and temperature profiles at an axial location $x = 1m$ are presented in Fig. 1. Axial distributions of heat transfer and skin friction are presented in Fig. 2. All of the present results show excellent correlation with the boundary layer predictions. As expected, equilibrium gas effects are not significant for this relatively low temperature flow.

Hypersonic Laminar Flat Plate Boundary Layer

The second test case consists of hypersonic laminar flow over a flat plate (this is also one of the test cases studied in [22]). The flow conditions are:

$$
\begin{aligned}
M_\infty &= 20.0 \\
Re_\infty / L &= 2.0 \cdot 10^5 / m \\
T_\infty &= 100.0\ ^\circ K \\
T_W &= 1000.0\ ^\circ K
\end{aligned}
$$

A grid consisting of 64 grid points in the streamwise direction and 64 grid points normal to the surface was employed. Average grid spacing normal to the surface was $0.1 \cdot 10^{-3}\ m$, producing an average y^+ of 1.08. The residual was reduced approximately 5 orders of magnitude over 4500 time steps. Reynolds execution times required for the three gas models were $4.4 \cdot 10^{-5}$, $8.8 \cdot 10^{-5}$, and $5.5 \cdot 10^{-5}$ cpu-seconds per mesh-cell-point per time-step-iteration, respectively.

Computed hypersonic laminar flat plate boundary layer results are compared to predictions made using CFL3DE, an extension of the CFL3D method by other investigators [23] which also incorporates equilibrium air effects (CFL3DE calculations supplied by Douglas Dilley, Analytical Services and Materials, Inc.). Velocity and temperature profiles at an axial location $x = 1m$ are presented in Fig. 3. Axial distributions of heat transfer, skin friction, and pressure are presented in Fig. 4. The present results show excellent correlation with the CFL3DE calculations. Equilibrium gas effects are significant, particularly for the temperature profile predictions.

High Speed Inlet

The third test case is the high speed flow through an inlet (this is also one of the test cases studied in [16]). The flow conditions are:

$$\begin{aligned} M_\infty &= 5.0 \\ Re_\infty/L &= 4.94 \cdot 10^6 / m \\ T_\infty &= 3573.0\ {}^\circ K \end{aligned}$$

The inlet features a 10° compression, followed downstream by a 10° expansion. Inviscid computations were obtained, to permit comparison with the exact perfect gas and equilibrium air solutions. A grid consisting of 201 grid points in the streamwise direction and 51 grid points normal to the surface was employed. The residual was reduced approximately 3 orders of magnitude over 3000 times steps. NASA Cray-2 (Navier) execution times required for the three gas models were $1.3 \cdot 10^{-4}$, $1.6 \cdot 10^{-4}$, and $1.3 \cdot 10^{-4}$ cpu-seconds per mesh-cell-point per time-step-iteration, respectively.

Computed high speed inlet results are compared to the exact inviscid solutions. Inlet-wall density, pressure, and temperature distributions appear in Fig. 5. The agreement is good, except for the temperature level aft of the expansion, which is overpredicted. The same effect is seen in [16]. No attempt was made to try to eliminate the post-shock oscillation evident in the present predictions, which nonetheless indicate the proper perfect gas/equilibrium air trends.

Calculations were also made using FVS. The residual was reduced 3.5 orders of magnitude over 3000 time steps. Navier execution times required for the three gas models were $8.1 \cdot 10^{-5}$, $1.2 \cdot 10^{-4}$, and $8.3 \cdot 10^{-5}$ cpu-seconds per mesh-cell-point per time-step-iteration, respectively. The results are shown in Fig. 6, and are similar to those obtained using FDS.

Bent Nose Biconic

The fourth test case is high speed laminar flow past a bent nose biconic (one of the test cases studied in [24]). The flow conditions are:

$$
\begin{aligned}
M_\infty &= 9.86 \\
Re_\infty / L &= 1.842 \cdot 10^6 / m \\
T_\infty &= 49.75\ ^\circ K \\
T_w &= 300.0\ ^\circ K
\end{aligned}
$$

As shown schematically in Fig. 7, a total of 85 grid points in the streamwise direction, 45 grid points normal to the surface, and 23 grid points circumferentially was used to model one-half of the configuration, with symmetry imposed across the x-z plane. Average grid spacing normal to the surface was $0.5 \cdot 10^{-5}\ m$, producing an average y^+ of 0.23. To avoid difficulties sometimes encountered using FDS to compute blunt nose flow fields, FVS was employed. The mesh sequencing capability was also used, to minimize overall execution time. The residual was reduced approximately 4.5 orders of magnitude over 4300 time steps. NASA Cray-2 (Voyager) execution times required for the three gas models were $7.0 \cdot 10^{-5}$, $9.9 \cdot 10^{-5}$, and $8.3 \cdot 10^{-5}$ cpu-seconds per mesh-cell-point per time-step-iteration, respectively.

Computed bent nose biconic surface heat transfer rates are compared to experimental data [25] in Fig. 8. The present results show good correlation with the data. Equilibrium gas effects are less significant than expected for this high speed flow.

Flared Cone (Laminar)

The fifth test case is that of high speed laminar flow past a flared cone (one of the test cases studied in [24]). The flow conditions are:

$$
\begin{aligned}
M_\infty &= 16.93 \\
Re_\infty / L &= 1.976 \cdot 10^5 \, / \, ft \\
T_\infty &= 83.73 \ ^\circ R \\
T_w &= 530.0 \ ^\circ R
\end{aligned}
$$

As shown schematically in Fig. 9, a total of 97 grid points in the streamwise direction, 45 grid points normal to the surface, and 19 grid points circumferentially was used to model one-half of the configuration, with symmetry imposed across the x-z plane. Average grid spacing normal to the surface was $0.24 \cdot 10^{-4} \, ft$, producing an average y^+ of 0.09. Employing the mesh sequencing capability, the residual was reduced approximately 3.5 orders of magnitude over 3100 time steps. Navier execution times required for the three gas models were $1.2 \cdot 10^{-4}$, $1.6 \cdot 10^{-4}$, and $1.5 \cdot 10^{-4}$ cpu-seconds per mesh-cell-point per time-step-iteration, respectively.

Computed flared cone surface heat transfer, skin friction, and pressure distributions for laminar flow are compared to experimental data [26] in Fig. 10. The present results show good correlation with the data. Equilibrium gas effects are less significant than expected for this high speed flow.

Flared Cone (Turbulent)

The sixth test case considered is high speed turbulent flow past a flared cone. The flow conditions are:

$$
\begin{aligned}
M_\infty &= 7.85 \\
Re_\infty / L &= 4.697 \cdot 10^6 \, / \, ft \\
T_\infty &= 130.2 \ ^\circ R \\
T_w &= 530.0 \ ^\circ R
\end{aligned}
$$

The grid, shown schematically in Fig. 11, is similar to that for the laminar case. Average grid spacing normal to the surface was $0.83 \cdot 10^{-5} \, ft$, producing an average y^+ of 0.51. The turbulence model was employed in the k-direction (normal to the body surface) only. As for the laminar case, mesh sequencing was employed, and the residual was reduced approximately 3.5 orders of magnitude over 3100 time steps. Voyager execution times required for the three gas models were $6.4 \cdot 10^{-5}$, $8.7 \cdot 10^{-5}$, and $7.2 \cdot 10^{-5}$ cpu-seconds per mesh-cell-point per time-step-iteration, respectively.

Computed flared cone surface heat transfer, skin friction, and pressure distributions for turbulent flow are compared to experimental data [26] in Fig. 12. The present results show good correlation with the data. The figure clearly indicates that appropriate use of the algebraic turbulence model can enhance code predictions.

Laminar Corner Flow

The seventh test case consists of laminar flow in a corner formed by two intersecting wedges (this flow is also studied in [27]). The flow conditions are:

$$
\begin{aligned}
M_\infty &= 3.0 \\
Re_\infty &= 2.22 \cdot 10^5 \\
T_\infty &= 105.0\ ^\circ K \\
T_w &= 294.0\ ^\circ K
\end{aligned}
$$

The flow was computed on a 120 by 120 crossflow plane grid, assuming conical flow in the streamwise direction. Average grid spacing normal to the surface was $0.14 \cdot 10^{-3}$ times x, producing an average y^+ of 6.05. Laminar viscous thin layer terms normal to both walls were included, in the j- and k-directions. The residual was reduced approximately 3 orders of magnitude over 3600 time steps. Navier execution times required for the three gas models were $7.8 \cdot 10^{-5}$, $1.2 \cdot 10^{-4}$, and $1.1 \cdot 10^{-4}$ cpu-seconds per mesh-cell-point per time-step-iteration, respectively.

Computed wall pressure distributions for laminar corner flow are compared to experimental data [28] in Fig. 13. The present results show good correlation with the data.

Turbulent Corner Flow

The eighth test case consists of turbulent corner flow (also studied in [27]). The flow conditions are:

$$
\begin{aligned}
M_\infty &= 3.0 \\
Re_\infty &= 3.03 \cdot 10^6 \\
T_\infty &= 105.0\ ^\circ K \\
T_w &= 294.0\ ^\circ K
\end{aligned}
$$

The flow was again computed on a 120 by 120 crossflow grid, and was assumed to be conical. Average grid spacing normal to the surface was $0.10 \cdot 10^{-3}$ times x, producing an average y^+ of 5.51. The two-wall corner model was used to simultaneously include turbulence effects normal to both walls, in the j- and k-directions. The residual was reduced approximately 4.5 orders of magnitude over 5400 time steps. Navier execution times required for the three gas models were $7.9 \cdot 10^{-5}$, $1.1 \cdot 10^{-4}$, and $1.1 \cdot 10^{-4}$ cpu-seconds per mesh-cell-point per time-step-iteration, respectively.

Computed wall pressure distributions for turbulent corner flow are compared to experimental data [28] in Fig. 14. The present results again show good correlation with the data. Compared to the previous laminar corner flow predictions, these results indicate that the proper trending is produced by use of the two-corner wall turbulence model.

CONCLUDING REMARKS

The results presented herein show good correlation for all of the test cases considered. Since the equilibrium gas flux splitting schemes make use of the "equivalent" specific heat ratios, $\tilde{\gamma}$ and Γ, which are stored in the q-vector as additional dependent variables, these results validate not only the implementation of the flux difference and flux vector splitting schemes, but also the restructuring of the present code to permit an arbitrary number of independent and dependent variables.

Both the Srinivasan and Tannehill equilibrium air model and the Liu and Vinokur generalized equilibrium gas model reproduce perfect gas results or, where appropriate, exhibit the proper real gas trends. With full vectorization, the equilibrium gas calculations were possible with only a small (~20%) increase in execution time. Successful coupling of the equilibrium air/equilibrium gas models with the one- or two-wall algebraic turbulence model was also demonstrated.

Although not all of the code's capabilities were exercised, the results are indicative of the success of a substantial portion of the current effort. The resulting method should prove to be a valuable tool for use by the National Aero-Space Plane program, as well as a good starting point for future efforts aimed at incorporating nonequilibrium/chemistry effects, more sophisticated turbulence and transition models, or a variety of other physical phenomena.

REFERENCES

[1] Thomas, J.L., and Newsome, R.W., "Navier-Stokes Computations of Lee-Side Flows over Delta Wings," AIAA Paper No. 86-1049, 1986.

[2] Thomas, J.L., Taylor, S.L., and Anderson, W.K., "Navier Stokes Computations of Vortical Flows Over Low Aspect Ratio Wings," AIAA Paper No. 87-0207, 1987.

[3] Vatsa, V.N., Thomas, J.L., and Wedan, B.W., "Navier-Stokes Computation of Prolate Spheroids at Angle of Attack," AIAA Paper No. 87-2627-CP, 1987.

[4] Ghaffari, F., Luckring, J.M., Thomas, J.L., and Bates, B.L., "Navier-Stokes Solutions about the F/A-18 Forebody-LEX Configuration," AIAA Paper No. 89-0338, 1989.

[5] Thomas, J.L., Van Leer, B., and Walters, R.W., "Implicit Flux-Split Schemes for the Euler Equations," AIAA Paper No. 85-1680, 1985.

[6] Van Leer, B., "Towards the Ultimate Conservative Difference Scheme: V. A Second-Order Sequel to Godunov's Method," *Journal of Computational Physics*, Vol. 32, No. 1, July 1979, pp. 101-136.

[7] Roe, P.L., "Approximate Riemann Solvers, Parameter Vectors, and Difference Schemes," *Journal of Computational Physics*, Vol. 43, 1981, pp. 357-372.

[8] Roe, P.L., "Characteristic Based Schemes for the Euler Equations," *Annual Review of Fluid Mechanics*, 1986.

[9] Van Leer, B., "Flux-Vector Splitting for the Euler Equations," ICASE Report No. 82-30, 1982.

[10] Baldwin, B.S., and Lomax, H., "Thin Layer Approximation and Algebraic Model for Separated Turbulent Flows," AIAA Paper No. 78-257, 1978.

[11] Walters, R.W., Reu, T., McGrory, W.D., Thomas, J.L., and Richardson, P.F., "A Longitudinally-Patched Grid Approach with Applications to High Speed Flows," AIAA Paper No. 88-0715, 1988.

[12] Anderson, W.K., Thomas, J.L., and Whitfield, D.L., "Three-Dimensional Multigrid Algorithms for the Flux-Split Euler Equations," NASA TP-2829, Nov. 1988.

[13] Jameson, A., and Baker, T.J., "Multigrid Solution of the Euler Equations for Aircraft Configurations," AIAA Paper No. 84-0093, 1984.

[14] Jameson, A., and Yoon, S., "Multigrid Solution of the Euler Equations Using Implicit Schemes," AIAA Paper No. 85-0293, 1985.

[15] Thomas, J.L., Walters, R.W., Ghaffari, F., Weston, R.P., and Luckring, J.M., "A Patched Grid Algorithm for Complex Configurations Directed Towards the F-18 Aircraft," AIAA Paper No. 89-0121, 1989.

[16] Grossman, B., and Walters, R.W., "An Analysis of Flux-Split Algorithms for Euler's Equations with Real Gases," AIAA Paper No. 87-1117-CP, 1988.

[17] Srinivasan, S., Tannehill, J.C., and Weilmunster, K.J., "Simplified Curve Fits for the Thermodynamic Properties of Equilibrium Air," NASA RP-1181, Aug. 1987.

[18] Liu, Y., and Vinokur, M., "Equilibrium Gas Flow Computations: I. Accurate and Efficient Calculation of Equilibrium Gas Properties," AIAA Paper No. 89-1736, 1989.

[19] Srinivasan, S., and Tannehill, J.C., "Simplified Curve Fits for the Transport Properties of Equilibrium Air," NASA CR-178411, Dec. 1987.

[20] Lawrence, S.L., Tannehill, J.C., and Chausee, D.S., "An Upwind Algorithm for the Parabolized Navier-Stokes Equations," AIAA Paper No. 86-1117, 1986.

[21] Harris, J.E., and Blanchard, D.K., "Computer Program for Solving Laminar, Transition, or Turbulent Compressible Boundary-Layer Equations for Two-Dimensional and Axisymmetric Flow," NASA TM-83207, Feb. 1982.

[22] Tannehill, J.C., Ievalts, J.O., and Lawrence, S.L., "An Upwind Parabolized Navier-Stokes Code for Real Gas Flows," AIAA Paper No. 88-0713, 1988.

[23] Walters, R.W., Dilley, A.D., Richardson, P.F., Thomas, J.L., and Grossman, B., "Hypersonic Real Gas Effects for an Upwind, Finite Volume 3-D Navier Stokes Code," Paper No. 90, 4th National Aero-Space Plane Symposium, Monterey, Feb. 1988.

[24] Wilson, G.J., and Davis, W.H., "Hypersonic Forebody Performance Sensitivity Studies Based on 3-D Equilibrium Navier-Stokes Calculations," AIAA Paper No. 88-0370, 1988.

[25] Miller, C.G., III, Micol, J.R., and Gnoffo, P.A., "Laminar Heat-Transfer Distributions on Biconics at Incidence in Hypersonic-Hypervelocity Flows," NASA TP-2213, 1985.

[26] Ryder, M.O., Jr., "Skin Friction, Heat Transfer, and Pressure Measurements on Hypersonic Inlet Compression Surfaces in the Mach Number Range 7.5 to 16," AFFDL TR-65-199, Dec. 1965.

[27] Rudy, D.H., Kumar, A., Thomas, J.L., Gnoffo, P.A., and Chakravarthy, S.R., "A Comparative Study and Validation of Upwind and Central-Difference Navier-Stokes Codes for High Speed Flows," Agard Symposium on Validation of Computational Fluid Dynamics, Lisbon, May 1988.

[28] West, J.E., and Korkegi, R.H., "Supersonic Interaction in the Corner of Intersecting Wedges at High Reynolds Numbers," *AIAA Journal*, Vol. 10, No. 5, May 1972, pp. 652-656.

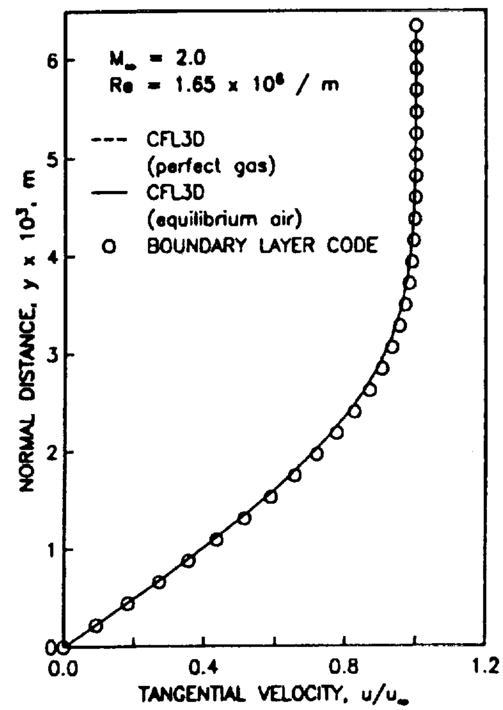

(a) Velocity

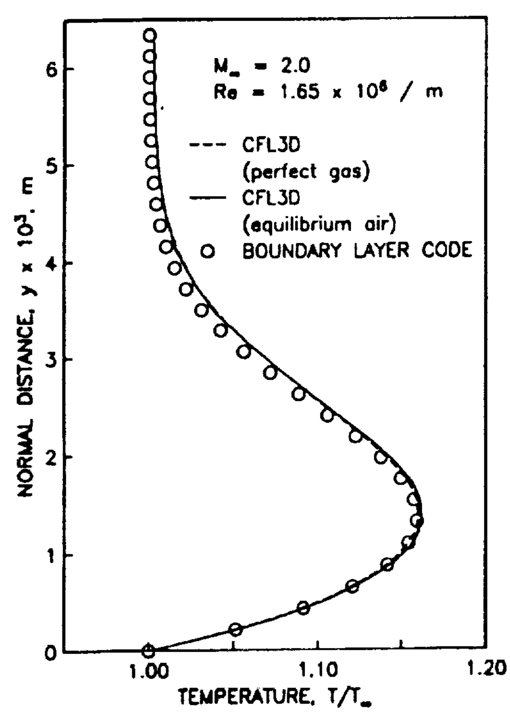

(b) Temperature

Figure 1: Supersonic Flat Plate Boundary Layer, Profiles at $x = 1m$.

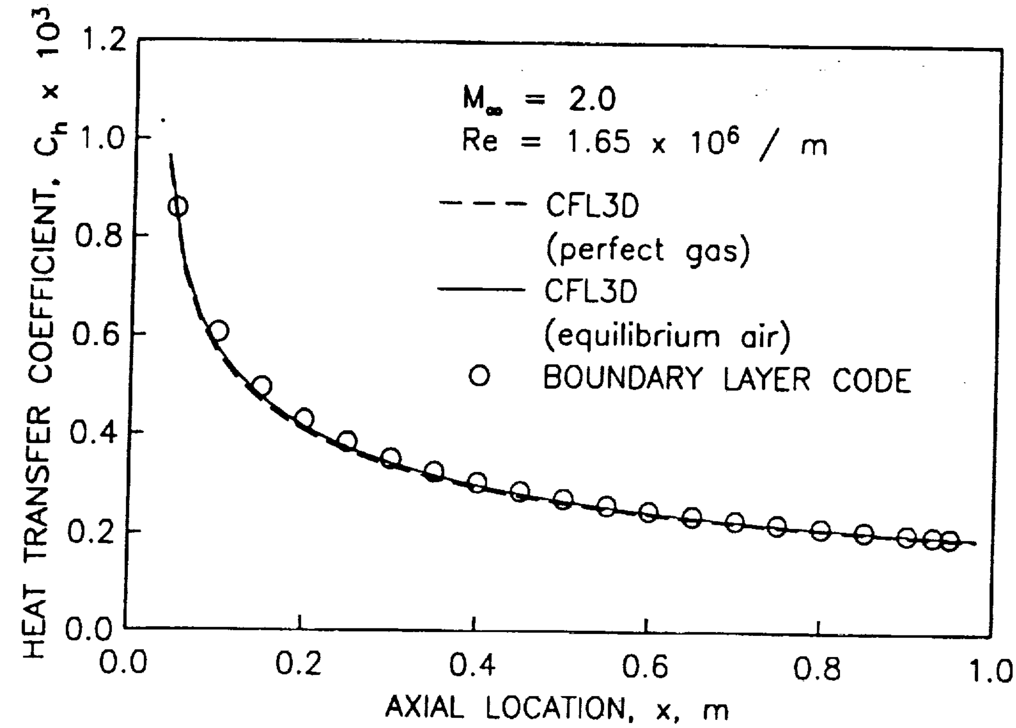

(a) Heat Transfer

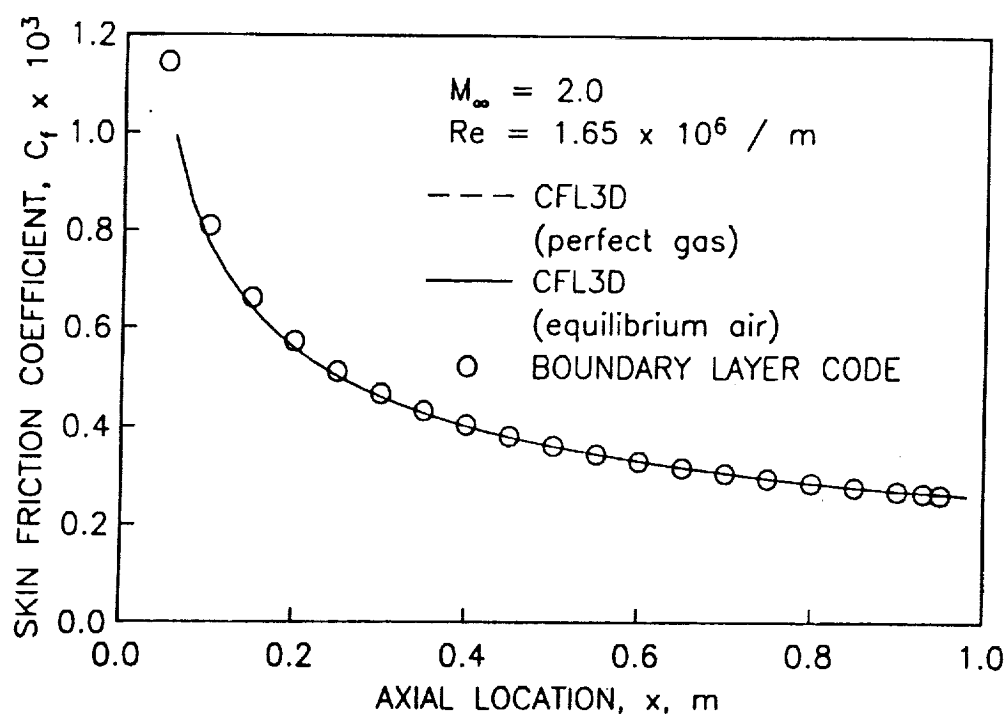

(b) Skin Friction

Figure 2: Supersonic Flat Plate Boundary Layer, Surface Distributions.

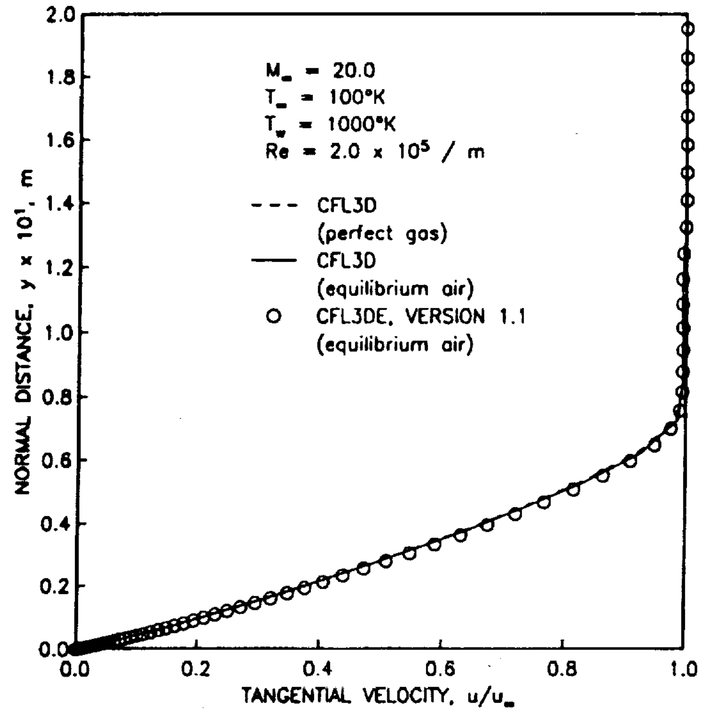

(a) Velocity

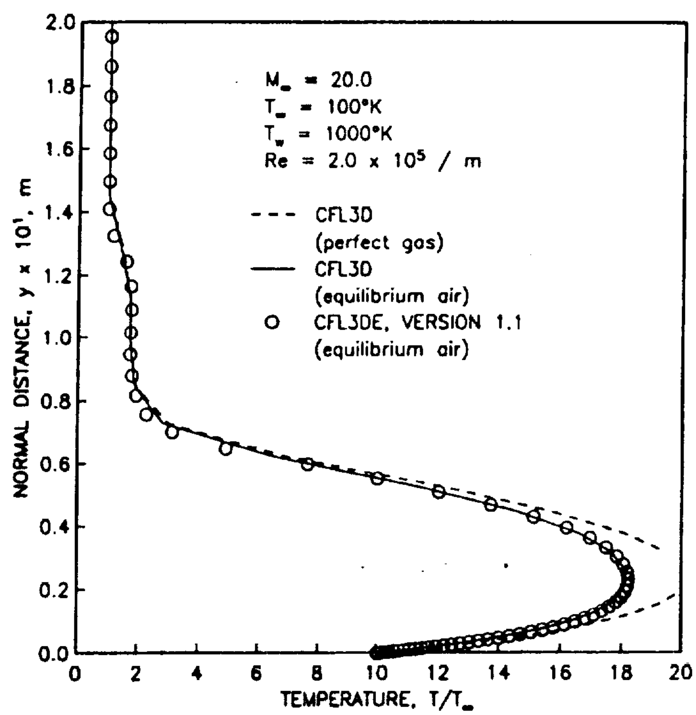

(b) Temperature

Figure 3: Hypersonic Flat Plate Boundary Layer, Profiles at $x = 1m$.

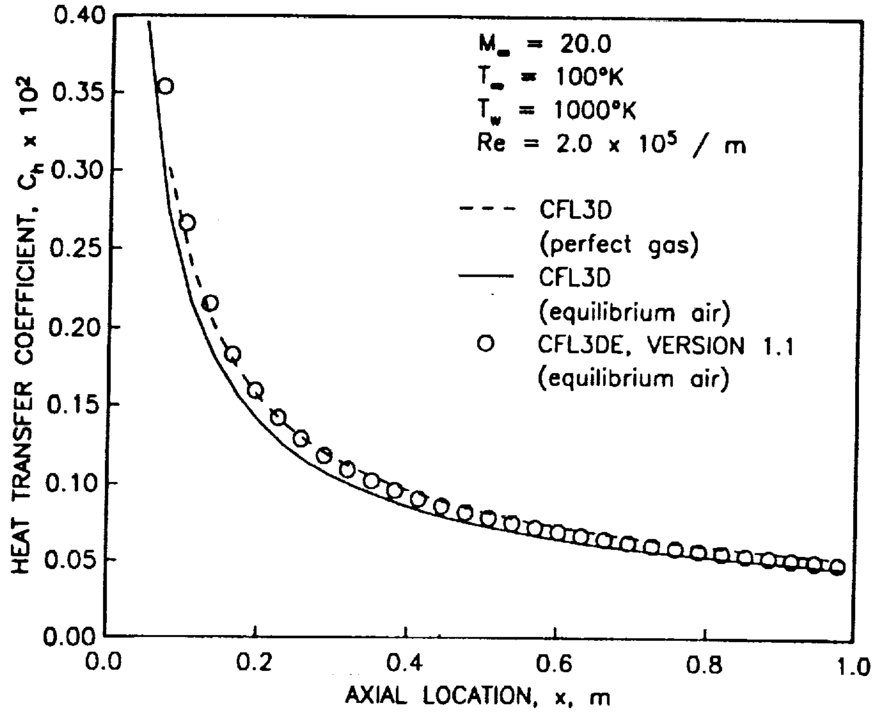

(a) Heat Transfer

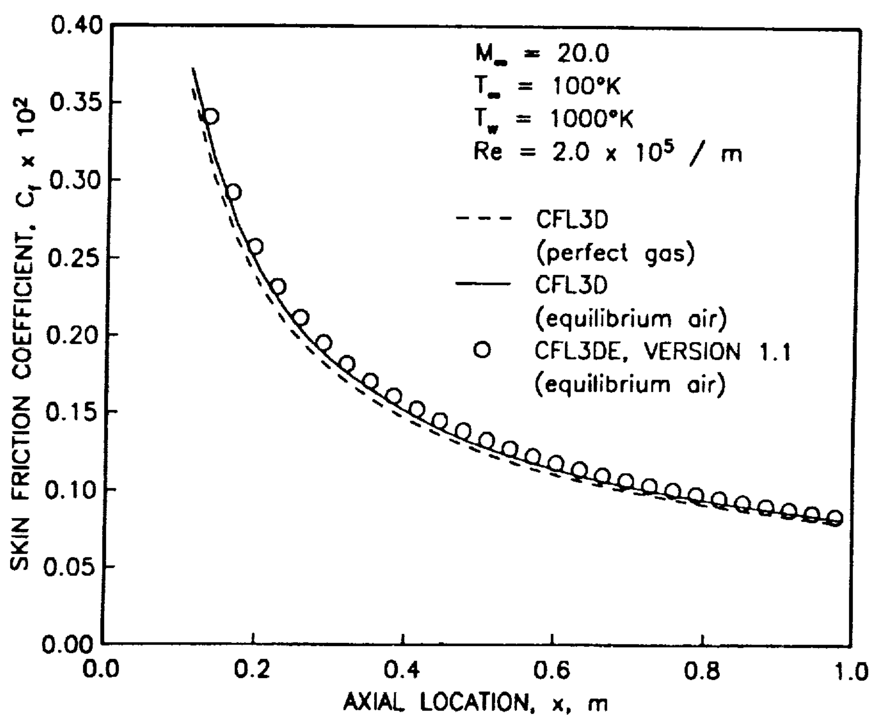

(b) Skin Friction

Figure 4: Hypersonic Flat Plate Boundary Layer, Surface Distributions.

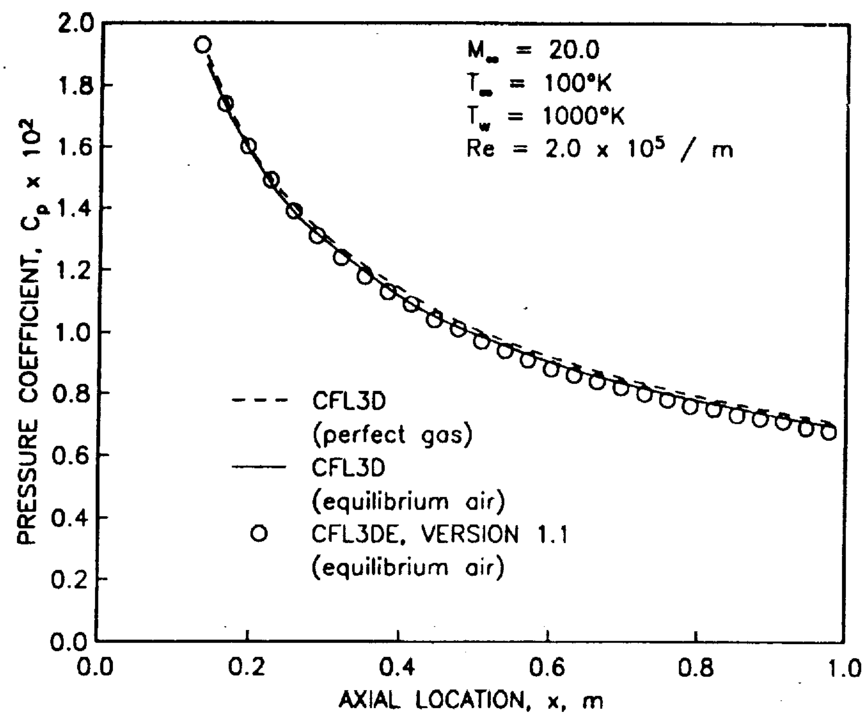

(c) Pressure

Figure 4: Hypersonic Flat Plate Boundary Layer, Surface Distributions (Conc'd).

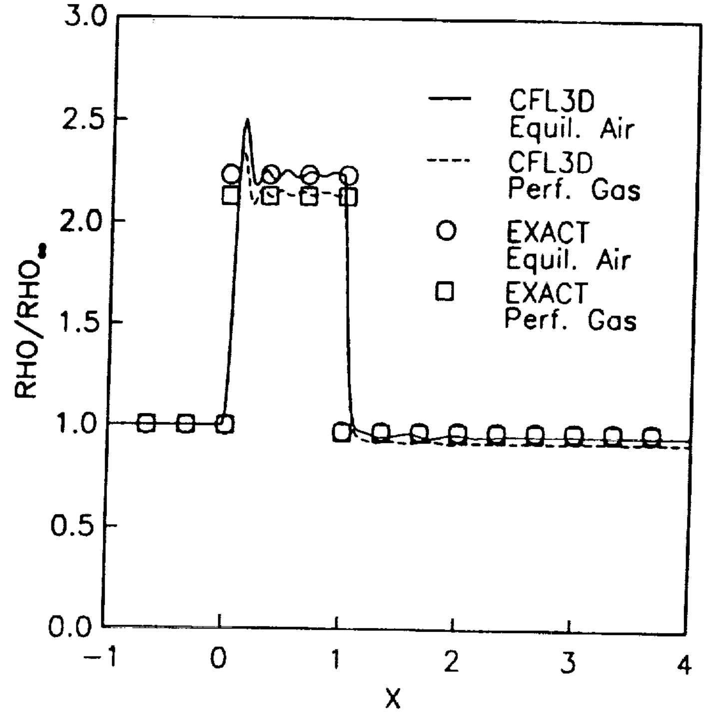

(a) Density

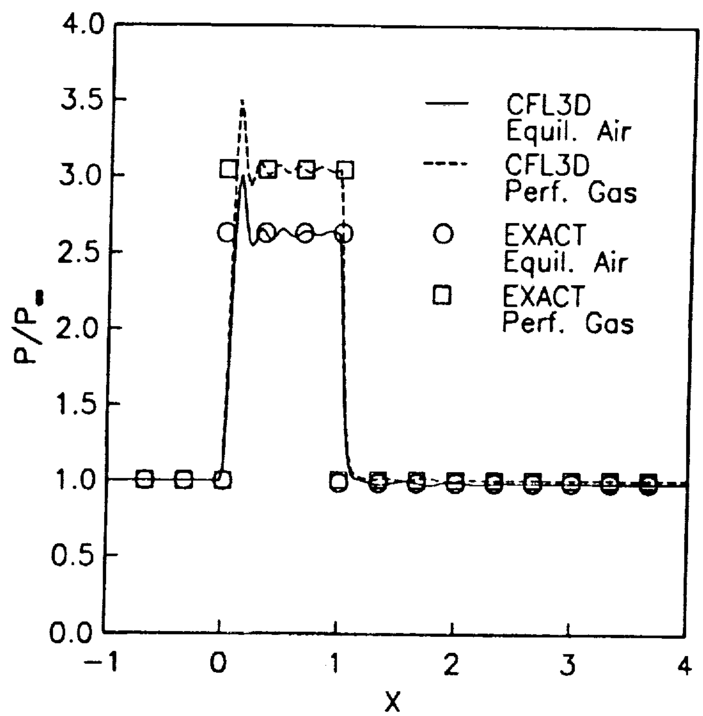

(b) Pressure

Figure 5: High Speed Inlet, Wall Distributions; Flux Difference Splitting.

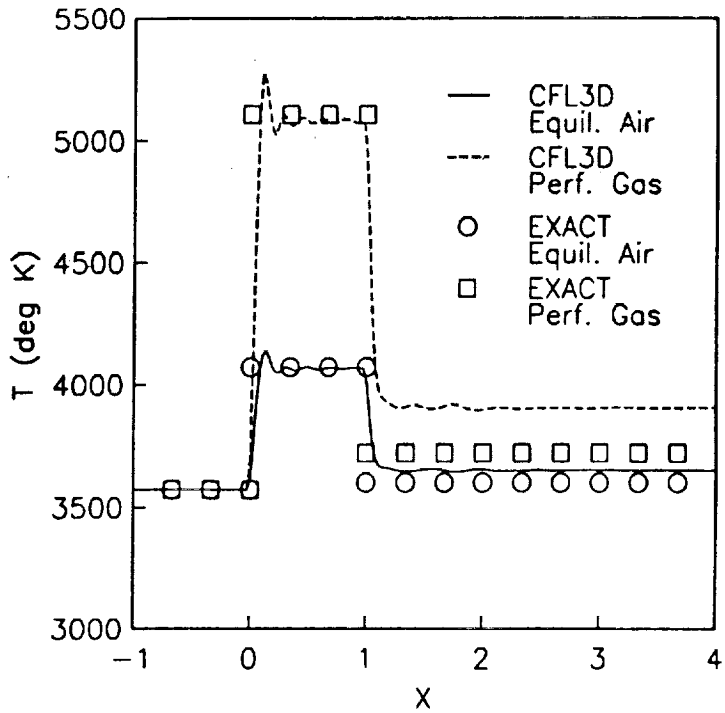

(c) Temperature

Figure 5: High Speed Inlet, Wall Distributions; Flux Difference Splitting (Conc'd).

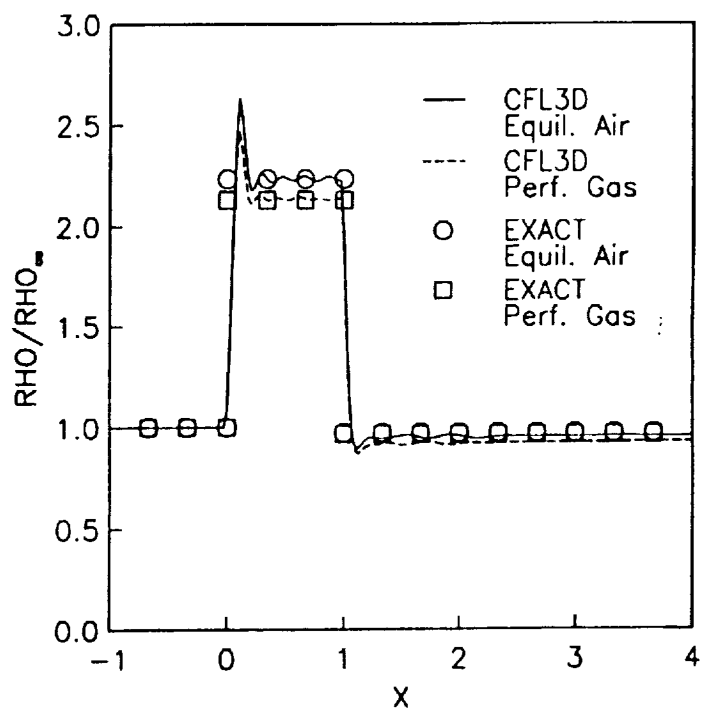

(a) Density

Figure 6: High Speed Inlet, Wall Distributions; Flux Vector Splitting.

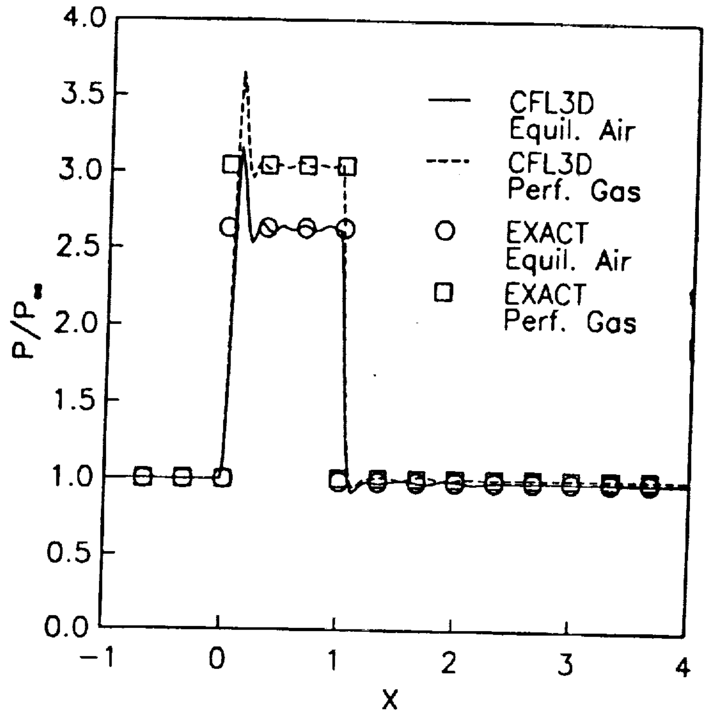

(b) Pressure

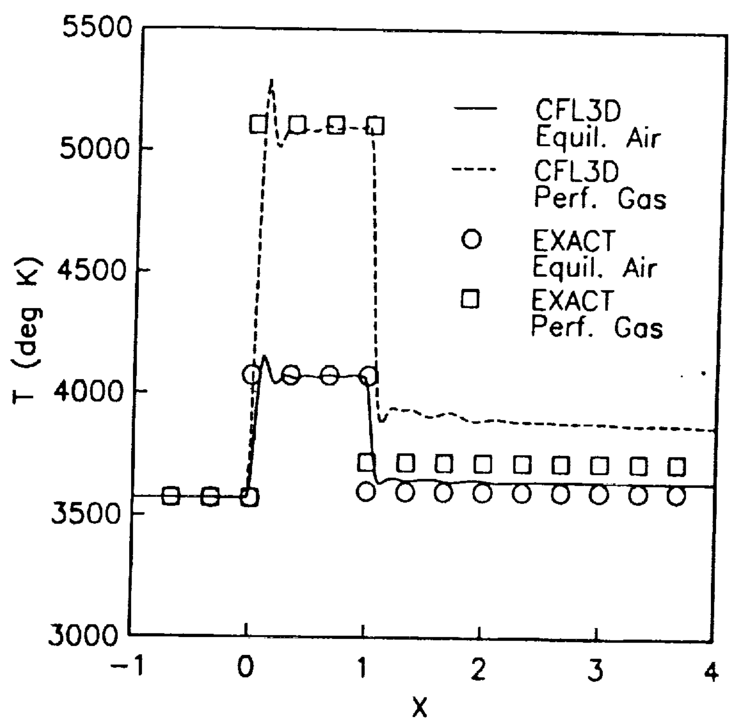

(c) Temperature

Figure 6: High Speed Inlet, Wall Distributions; Flux Vector Splitting (Conc'd).

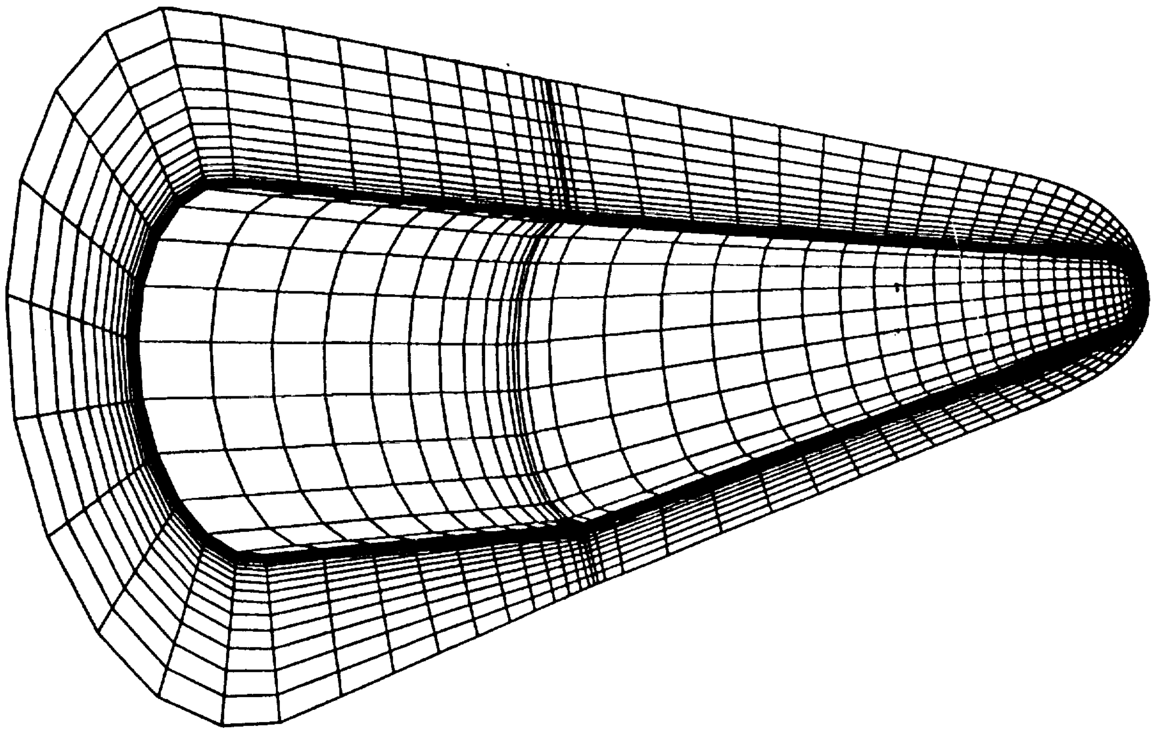

Figure 7: Schematic of Computational Grid for Bent Nose Biconic.

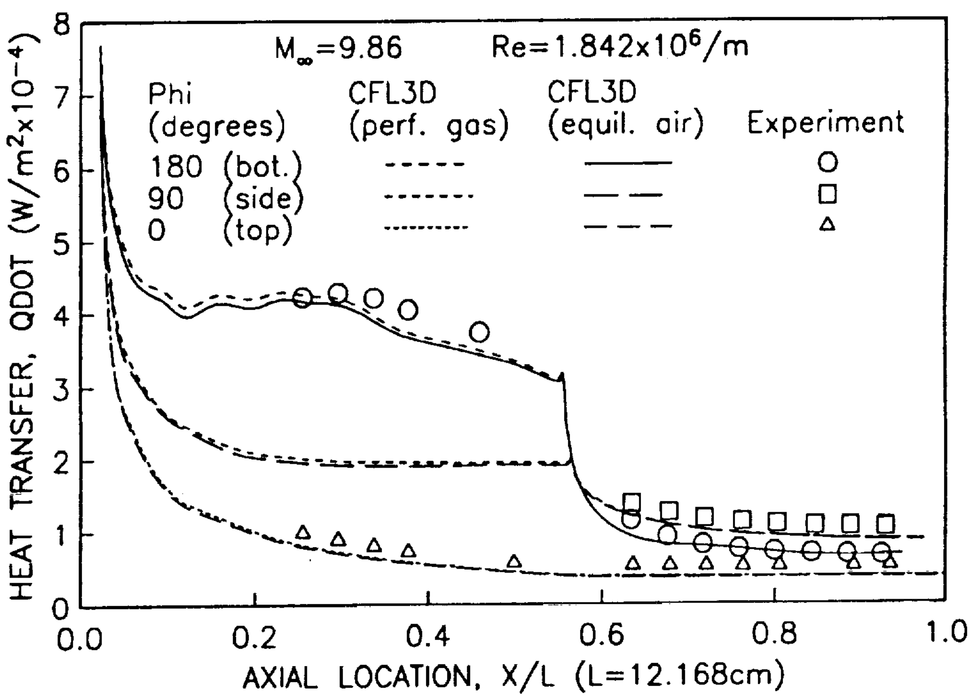

Figure 8: Bent Nose Biconic, Surface Heat Transfer Distribution.

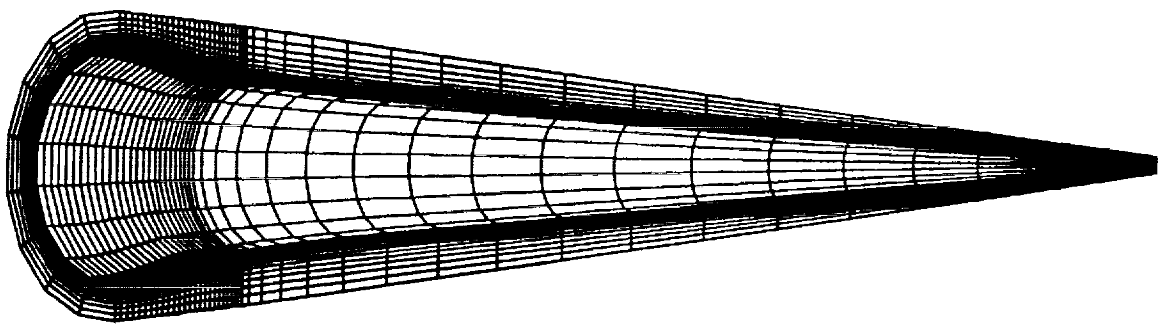

Figure 9: Schematic of Computational Grid for Flared Cone; Laminar Flow.

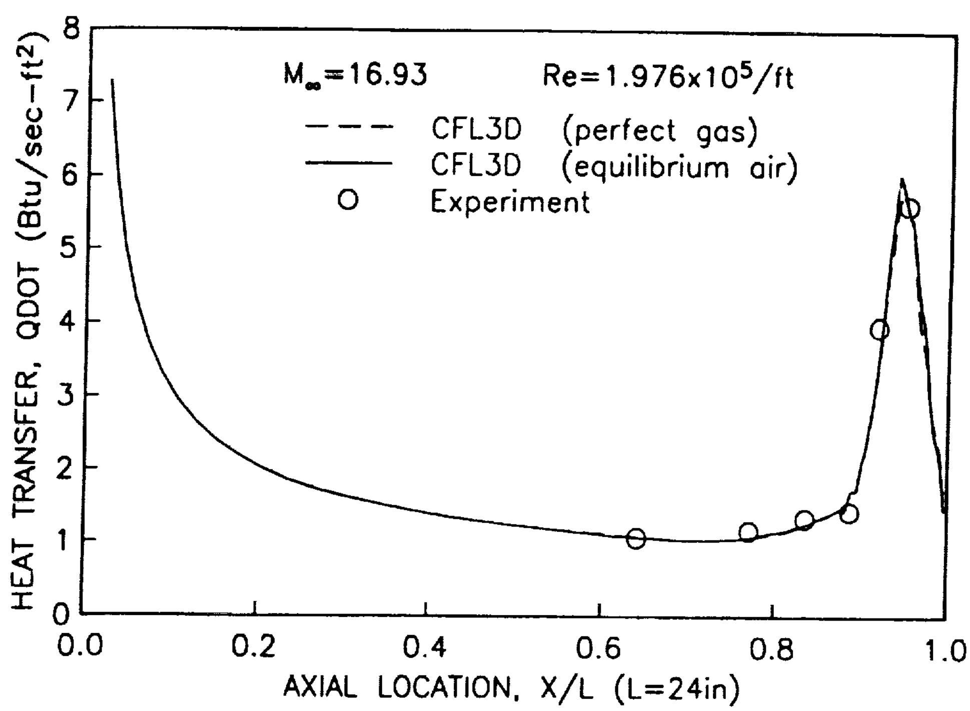

(a) Heat Transfer

Figure 10: Flared Cone, Surface Distributions; Laminar Flow.

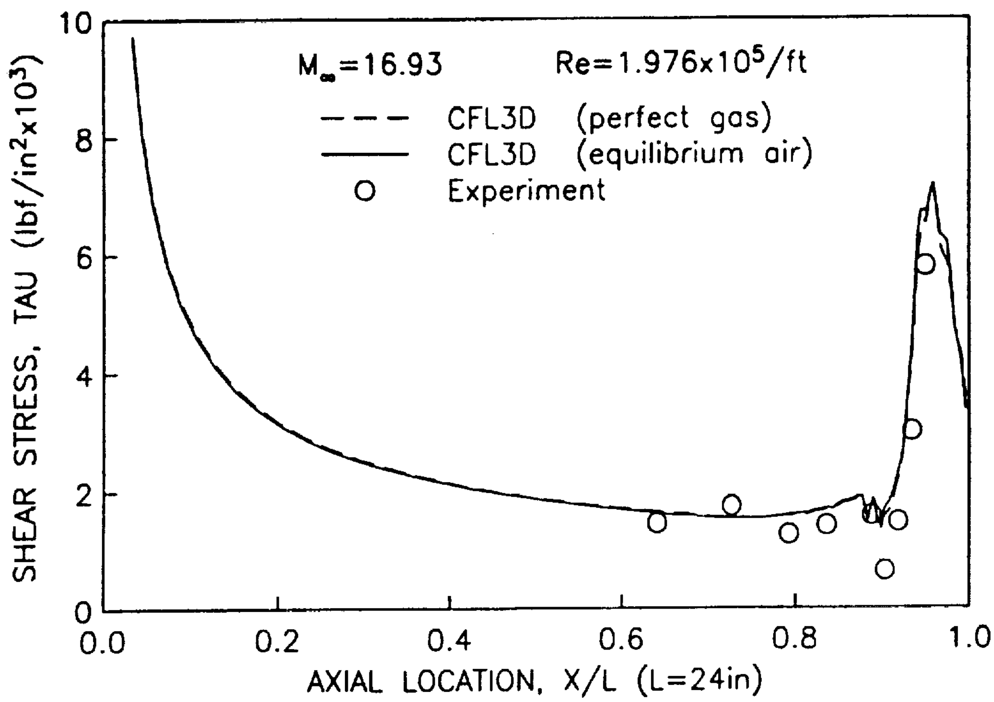

(b) Shear Stress

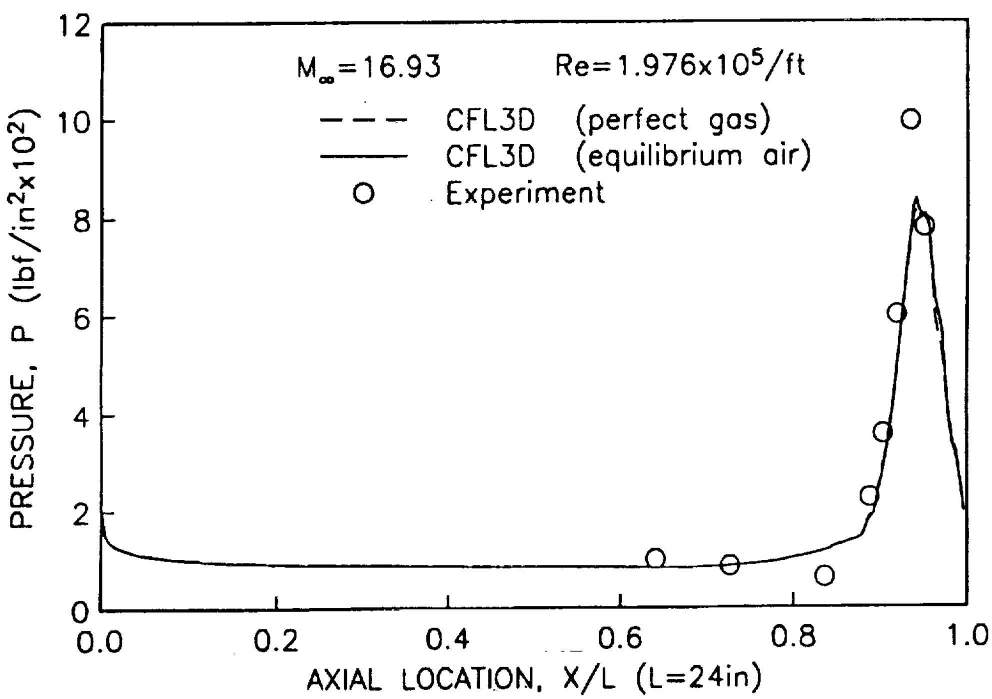

(c) Pressure

Figure 10: Flared Cone, Surface Distributions; Laminar Flow (Conc'd).

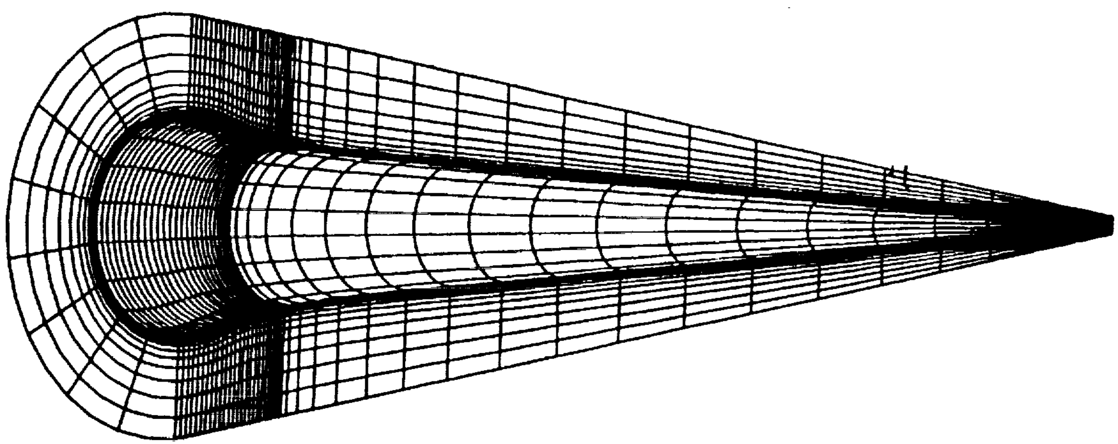

Figure 11: Schematic of Computational Grid for Flared Cone; Turbulent Flow.

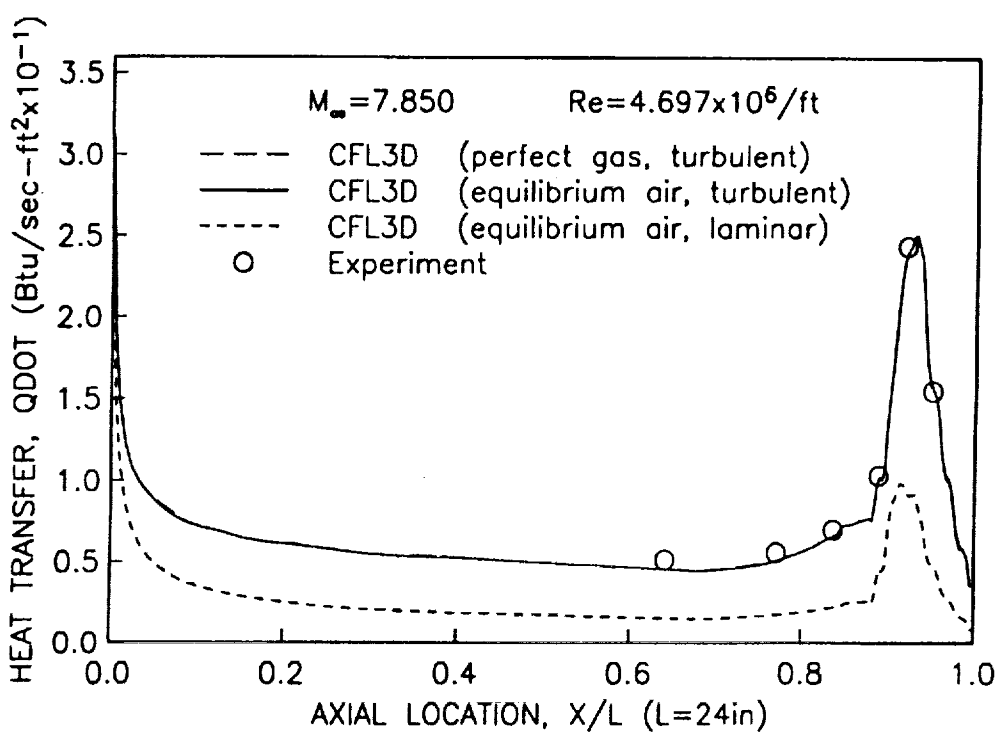

(a) Heat Transfer

Figure 12: Flared Cone, Surface Distributions; Turbulent Flow.

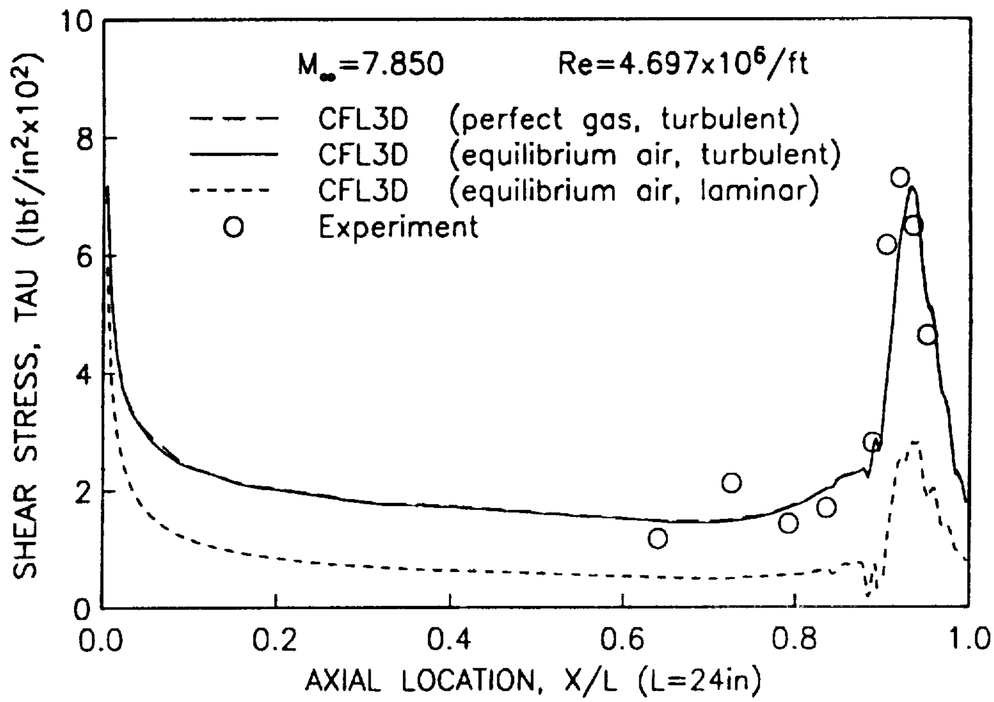

(b) Shear Stress

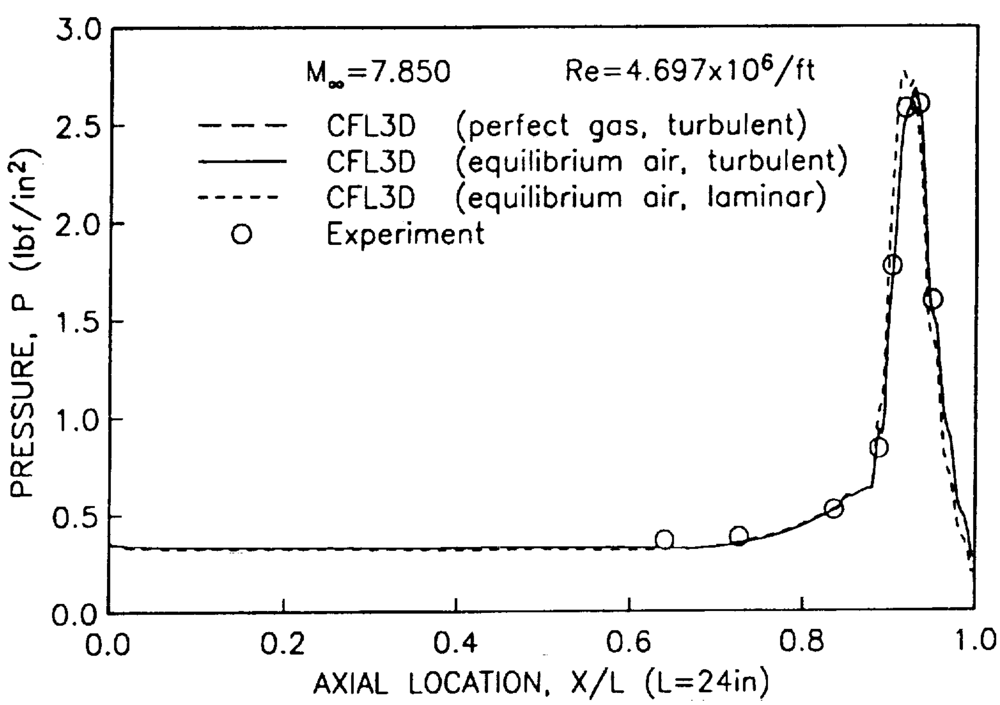

(c) Pressure

Figure 12: Flared Cone, Surface Distributions; Turbulent Flow (Conc'd).

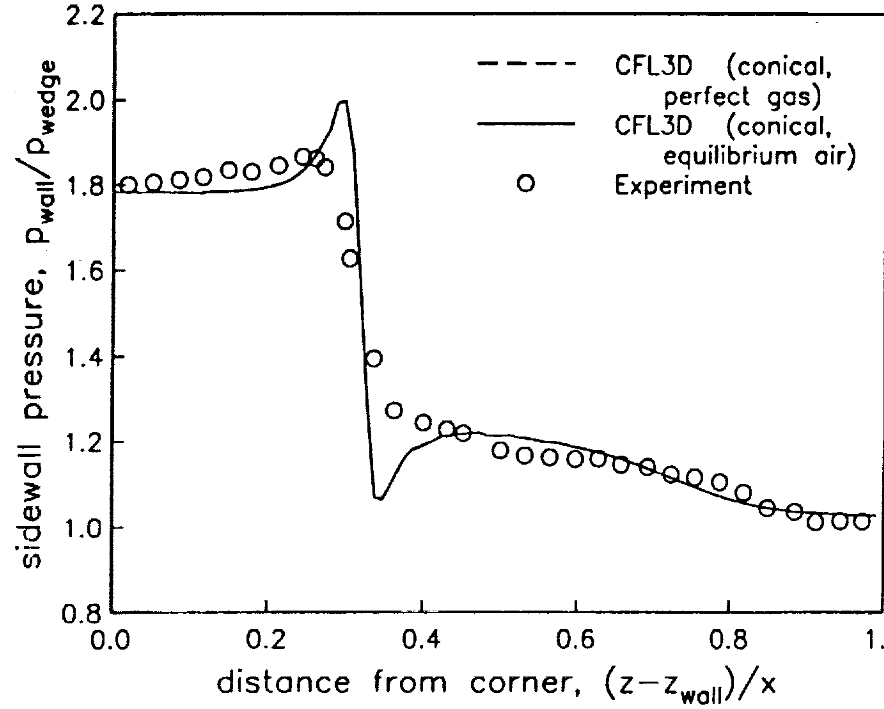

Figure 13: Laminar Corner Flow, Wall Pressure Distribution.

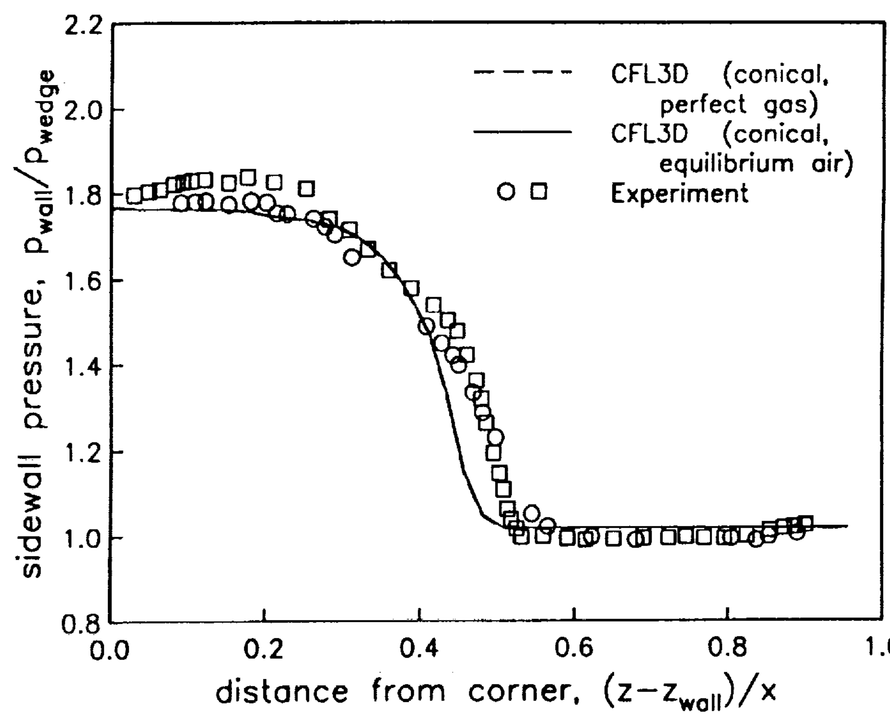

Figure 14: Turbulent Corner Flow, Wall Pressure Distribution.

APPENDIX A

Modified CFL3D Input Data File Description

```
****************************** LINE TYPE ONE ******************************

   title describing case

*************************** LINE TYPE ONE.FIVE ***************************
         (DATA FOR LINE TYPE ONE.FIVE REPEATED FOR EACH FILE)

   path/name of binary grid file              (unit 01)

   path/name of binary restart file           (unit 02)

   path/name of binary PLOT3D grid file       (unit 03)

   path/name of binary PLOT3D flowfield file  (unit 04)

   path/name of binary Liu & Vinokur equilibrium air coefficient file
                                              (unit 07)

   path/name of primary output file           (unit 11)

   path/name of FIXI/FIXJ output file         (unit 12)

   path/name of wing pressure output file     (unit 14)

   path/name of secondary output file         (unit 15)

   path/name of flowfield output file         (unit 17)

   path/name of unsteady cp output file       (unit 20)

****************************** LINE TYPE TWO ******************************

   xmach - freestream Mach number

   alpha - angle of attack

   beta  - side-slip angle

   reue  - freestream Reynolds number per unit length (millions)

   tinf  - freestream temperature (degrees Rankine)

   isnd  - wall temperature boundary condition flag
         = 0  adiabatic wall temperature
         = 1  specified wall temperature

   c2spe - wall temperature (temperature at wall divided by tmperature
                             of freestream)
           if c2spe<=0, c2spe taken as freestream stagnation temperature)

***************************** LINE TYPE THREE *****************************

   sref - reference area

   cref - reference length

   bref - reference span

   xmc  - moment center in x-direction
```

```
ymc   - moment center in y-direction

zmc   - moment center in z-direction

************************** LINE TYPE THREE.FIVE *****************************

igas    - perfect gas/equilibrium air flag
        = 1  perfect gas
        = 2  Tannehill equilibrium air
        = 3  Liu & Vinokur equilibrium air

gamma   - perfect gas, ratio of specific heats

rgas    - perfect gas, gas constant

prgas   - perfect gas, prandtl number

scalex - meters per unit length
        = 1.0 if using meters
        = 0.3048 if using feet, default
        = 0.02540 if using inches

scalet - degrees Kelvin per unit degree
        = 1.0 if using degrees Kelvin
        = 0.5556 if using degrees Rankine, default

scalem - kilograms per unit mass
        = 1.0 if using kilograms
        = 14.59 if using slugs, default
        = 0.453472 if using pounds (mass)

****************************** LINE TYPE FOUR *****************************

dt - time step
    < 0  local time stepping, CFL=abs(dt)
    > 0  constant time step  (=dt)

irest    = 0  no restart
         = 1  restart

iflagts = 0  constant dt
        > 0  dt ramped over iflagts steps to dt*fmax

fmax - maximum increase in dt

iunst = 0  steady
      = 1  sinusoidal plunging
      = 2  sinusoidal pitching

rfreq  - reduced frequency

alphau - pitching alpha

cloc   - pitching center

****************************** LINE TYPE FIVE ******************************

ngrid   - number of grids input

nplot3d - number of flowfield data sets to be written in
          plot3d format
```

```
nprint  - number of data sets to be sent to an output file

nwrest  - number of iterations between updates of the binary
           restart file


***************************** LINE TYPE SIX *****************************
               (DATA FOR LINE TYPE SIX REPEATED NGRID TIMES)

ncg  - number of coarser grids to construct for multigrid/mesh
        sequencing  (= 0 for embedded mesh)

iem  - embedded mesh flag
     = 0 for global grid
     = 1 level of this embedded grid above global grid level

iadvance - flag to skip any residual/update calculations
         >=0  proceed as usual
         < 0  skip residual/update calculations

iforce  -  flag to skip the force routine
        >=0  proceed as usual
        < 0  skip force calculations

imesh - mesh flag for grids topologically similar to:
      =  0  no singularties in mesh
      =  1  delta wing   (AIAA 87-0207)
      =  2  prolate spheroid   (AIAA 87-2627CP)
      =  3  prolate spheroid with sting   (AIAA 87-2627CP)
      = 10  wing (o-h)
      = 11  wing (c-h)   (AIAA 86-0274)
      = 12  wing (c-o)   (AIAA 86-0274)

ivisc(m) - viscous/inviscid interaction flag   m= 1 : I-direction
        = 0  inviscid                             2 : J-direction
        = 1  laminar                              3 : K-direction
        = 2  turbulent

NOTE:  The thin layer viscous terms can be included in either the
       j-, k-, or i-directions, separately.  The viscous terms can
       be included simultaneously in, at most, two directions,
       either j-k or i-k, for any particular grid.  It is prefer-
       able to let k be the primary viscous direction and j be the
       secondary viscous direction.


***************************** LINE TYPE SEVEN *****************************
              (DATA FOR LINE TYPE SEVEN REPEATED NGRID TIMES)

grid dimensions:
idim - number of points in i-direction
     * for imesh = 1      axial direction (along chord)      (h-mesh)
     * for imesh = 2      circumferentially along body       (o-mesh)
     * for imesh = 3      cir. along body/sting              (c-mesh)
     * for imesh = 10,11  spanwise direction                 (h-mesh)
     * for imesh = 12     spanwise:wrapping around wing tip  (o-mesh)

jdim - number of points in j-direction
     * for imesh = 1,2,3  circumferentially along body/wing  (c-mesh)
     * for imesh = 10     circumferentially along chord      (o-mesh)
     * for imesh = 11,12  cir. along wing chord and wake     (c-mesh)

kdim - number of points in k-direction
     * for all imesh, radial direction

itel - i location on body
```

```
     = i at apex                                   for imesh = 1
     = 1                                           for imesh = 2,3,10,11,12

ite2 - i location on body
     = i at trailing edge                          for imesh = 1
     = idim                                        for imesh = 2,3,12
     = i at wing tip                               for imesh = 10,11

jte1 - j location on body
     = 1                                           for imesh = 1,2,3,10
     = j at trailing edge on lower surface         for imesh = 11,12

jte2 - j location on body
     = jdim                                        for imesh = 1,2,3,10
     = j at trailing edge on upper surface         for imesh = 11,12

**************************** LINE TYPE EIGHT ******************************
             (DATA FOR LINE TYPE EIGHT REPEATED NGRID TIMES)

inewg - restart flag for grid (not needed if irest=0)
      = 0  read flowfield data from restart file
      = 1  initialize at freestream or by linear interpolation
            from coarser grids

igridc - grid to which this grid connects (input 0 for global
         mesh(iem=0) and the grid number in which the embedded
         mesh fits for embedded meshes(iem>0))

js,ks,is - starting indices in connecting grid for placement of
           embedded mesh (input 0 for global meshes)

je,ke,ie - ending indices in connecting grid for placement of
           embedded mesh (input 0 for global meshes)

NOTE:  The embedded meshes must be a regular refinement in all
       directions of the grid to which it connects.

***************************** LINE TYPE NINE ******************************
             (DATA FOR LINE TYPE NINE REPEATED NGRID TIMES)

idiag(m) - matrix inversion flag
         = 0  5x5 block tridiagonal inversion
         = 1  scalar tridiagonal inversions (recommended)

iflim(m) - flux limiter flag                      m=1 : I-direction
         = 0  unlimited                            =2 : J-direction
         = 1  smooth limiter                       =3 : K-direction
         = 2  min-mod scheme (recommended)

****************************** LINE TYPE TEN ******************************
             (DATA FOR LINE TYPE TEN REPEATED NGRID TIMES)

ifds(m)  - spatial differencing parameter for Euler fluxes
         = 0  flux-vector splitting
         = 1  flux-difference splitting (Roe's scheme) (recommended)

rkap0(m) - spatial differencing parameter for Euler fluxes
         =  -1  fully upwind
         =   0  Frommes's scheme
         =   1  central
         = 1/3  upwind-biased third order (recommended)
```

****************************** LINE TYPE ELEVEN ******************************
(DATA FOR LINE TYPE ELEVEN REPEATED NGRID TIMES)

```
boundary condition flags:
mtypei(1) - boundary flag for i=0 boundary
mtypei(2) - boundary flag for i=idim boundary
mtypej(1) - boundary flag for j=0 boundary
mtypej(2) - boundary flag for j=jdim boundary
mtypek(1) - boundary flag for k=0 boundary
mtypek(2) - boundary flag for k=kdim boundary
```

NOTE: Particular choices of mtypei/j/k determine the type of boundary conditions used at the edges of the computational grids and are best determined by inspection of subroutine BC. Additional boundary condition types can be incorporated into the algorithm by modifying subroutine BC according to the conventions outlined there.

**************************** LINE TYPE ELEVEN.ONE ****************************

```
nbli    - number of block boundary conditions
```

**************************** LINE TYPE ELEVEN.TWO ****************************
(DATA FOR LINE TYPE ELEVEN.TWO REPEATED NBLI TIMES)

```
nblon   - block boundary condition on or off ( >=0 or <0 )
```

*************************** LINE TYPE ELEVEN.THREE ***************************
(DATA FOR LINE TYPE ELEVEN.THREE REPEATED NBLI TIMES)

```
blck1   - first block involved in block interface nbli
ist     - starting i-indice for blck1 interface
jst     - starting j-indice for blck1 interface
kst     - starting k-indice for blck1 interface
ind     - ending i-indice for blck1 interface
jnd     - ending j-indice for blck1 interface
knd     - ending k-indice for blck1 interface
ind1    - first indice which varies along blck1 interface
          ( 1=i ; 2=j ; 3=k )
ind2    - second indice which varies along blck1 interface
          ( 1=i ; 2=j ; 3=k )
blck2   - second block involved in block interface nbli
ist     - starting i-indice for blck2 interface
jst     - starting j-indice for blck2 interface
kst     - starting k-indice for blck2 interface
ind     - ending i-indice for blck2 interface
jnd     - ending j-indice for blck2 interface
knd     - ending k-indice for blck2 interface
ind1    - first indice which varies along blck2 interface
          ( 1=i ; 2=j ; 3=k )
ind2    - second indice which varies along blck2 interface
          ( 1=i ; 2=j ; 3=k )
```

****************************** LINE TYPE TWELVE ******************************

```
mseq    - mesh sequencing flag for global grids (maximum 5)
        = 1  single solution on finest grid
        = 2  solution on second finest grid advanced ncyc(1) cycles
             followed by ncyc(2) cycles on finest grid.  The solu-
             tion on the finest grid is obtained by interpolation
             from the coarser grid.  If ncyc(2)=0, solution
             terminated on second finest grid after ncyc(1) steps
```

```
                with restart file written for second finest grid at
                that point.
            > 2 sequencing from coarest to finest mesh as above

   mgflag - multigrid flag
            = 0 no multigrid
            = 1 multigrid on coarser global meshes
            = 2 multigrid on coarser global meshes and on
                 embedded meshes

   iconsf - conservation flag
            = 0 nonconservative flux treatment for embedded grids
            = 1 conservative flux treatment for embedded grids

   mtt      = 0 no additional iterations on the "up" portion
                of the multigrid cycle
            > 0 mtt additional iterations on the "up" portion
                of the multigrid cycle

   ngam - multigrid cycle flag
          = 1 V-cycle
          = 2 W-cycle
```

```
**************************** LINE TYPE THIRTEEN ***************************
   (REPEATED FOR EACH SEQUENCE 1 THROUGH MSEQ (COARSEST TO FINEST))

   ncycl  - number of cycles
   mglevg - number of grids to use in multigrid cycling for
            the global meshes
          = 1 for single grid
          = 2 for two levels
          = m for m levels
   nemgl  - number of embedded grid levels above the finest
            global grid (= 0 for global grids coarser than the
            finest global grid)
          = 0 no embedded grids
          = 1 one embedded grid
          = m m embedded grids
   nitfol - number of first order iterations
```

```
**************************** LINE TYPE FOURTEEN ***************************
    (REPEATED FOR EACH SEQUENCE 1 THROUGH MSEQ (COARSEST TO FINEST))

   mitL   - iterations on level L for each level L from coarsest
             to finest (mitL=1 recommended)
```

```
**************************** LINE TYPE FIFTEEN ****************************
                          (REPEATED NPLOT3D TIMES)

  block - designated block number for output
  istart - starting location in i-direction
  iend   - ending location in i-direction
  iinc   - increment factor in i-direction
  jstart - starting location in j-direction
  jend   - ending location in j-direction
  jinc   - increment factor in j-direction
  kstart - starting location in k-direction
  kend   - ending location in k-direction
  kinc   - increment factor in k-direction
```

```
**************************** LINE TYPE SIXTEEN ****************************
                          (REPEATED NPRINT TIMES)
```

```
block - designated block number for output
istart - starting location in i-direction
iend   - ending location in i-direction
iinc   - increment factor in i-direction
jstart - starting location in j-direction
jend   - ending location in j-direction
jinc   - increment factor in j-direction
kstart - starting location in k-direction
kend   - ending location in k-direction
kinc   - increment factor in k-direction
```

APPENDIX B

Sample Modified CFL3D Input Data Files

Supersonic Laminar Flat Plate Boundary Layer

```
   2-d plate, cfl3dn - liu,lam
binary grid file
   '/scr6/rosen/plt32/plt32.grd'
binary restart file
   '/scr6/rosen/plt32/plt32c.bin'
plot3d binary grid file
   '/scr6/rosen/plt32/plt32c.plg'
plot3d binary flowfield file
   '/scr6/rosen/plt32/plt32c.plq'
Liu & Vinokur binary equilibrium air coefficient file
   '/scr6/rosen/cfl3dn/liu/liubsr.cof'
primary output file
   '/scr6/rosen/plt32/plt32c.out'
fixi/fixj output file
   '/scr6/rosen/plt32/plt32c.fix'
wing pressure output file
   '/scr6/rosen/plt32/plt32c.wng'
secondary output file
   '/scr6/rosen/plt32/plt32c.sec'
flowfield output file
   '/scr6/rosen/plt32/plt32c.prt'
unsteady cp output file
   '/scr6/rosen/plt32/plt32c.ucp'
     XMACH     ALPHA      BETA  REUE,MIL    TINF,dK      ISND      C2SPE
      2.00     0.000       0.0  1.650000     221.60         1     1.0000
      SREF      CREF      BREF       XMC        YMC       ZMC
    1.0000    1.0000    1.0000        0.         0.        0.
      IGAS     GAMMA      RGAS     PRGAS     SCALEX    SCALET     SCALEM
         3       1.4     286.9      0.72        1.0       1.0        1.0
        DT     IREST  IFLAGTS       FMAX      IUNST     RFREQ     ALPHAU       CLOC
    -0.001         0       500     10.00          0   0.00000    0.00000    0.00000
     NGRID   NPLOT3D    NPRINT    NWREST
         1         0         2       100
       NCG       IEM  IADVANCE    IFORCE      IMESH  IVISC(I)   IVISC(J)   IVISC(K)
         0         0         0         0          0         0          0          1
      IDIM      JDIM      KDIM      ITE1       ITE2      JTE1       JTE2
         2        51       100         1          2         1         51
     INEWG    IGRIDC        IS        JS         KS        IE         JE         KE
         1         0         0         0          0         0          0          0
   IDIAG(I)  IDIAG(J)  IDIAG(K)  IFLIM(I)   IFLIM(J)  IFLIM(K)
         0         0         0         2          2         2
    IFDS(I)   IFDS(J)   IFDS(K)  RKAP0(I)   RKAP0(J)  RKAP0(K)
         1         1         1   0.33333    0.33333   0.33333
 MTYPEI(1) MTYPEI(2) MTYPEJ(1) MTYPEJ(2) MTYPEK(1) MTYPEK(2)
        11        11        27        27         67        67
 NUMBER OF BLOCK INTERFACE BOUNDARY CONDITIONS
   0
 BLOCK INTERFACE BOUNDARY CONDITION ON OR OFF ( >=0 OR <0 )
 BLCK1 IST JST KST IND JND KND IND1 IND2 BLCK2 IST JST KST IND JND KND IND1 IND2
      MSEQ    MGFLAG    ICONSF       MTT       NGAM
         1         0         0         0         01
      NCYC    MGLEVG     NEMGL     NITFO
       500        01        00       000
      MIT1      MIT2      MIT3      MIT4       MIT5
        01        01        01        01         01
  PRINT OUT:
  BLOCK ISTART    IEND    IINC JSTART    JEND    JINC KSTART    KEND    KINC
      1      1       1       1     50      50       1      1      99       1
      1      1       1       1      2      50       1      1       1       1
```

Hypersonic Laminar Flat Plate Boundary Layer

```
   2-d plate, cfl3dn : liu,lam
binary grid file
   '/scr6/rosen/plt20/plt20.grd'
binary restart file
   '/scr6/rosen/plt20/plt20c.bin'
plot3d binary grid file
   '/scr6/rosen/plt20/plt20c.plg'
plot3d binary flowfield file
   '/scr6/rosen/plt20/plt20c.plq'
Liu & Vinokur binary equilibrium air coefficient file
   '/scr6/rosen/cfl3dn/liu/liubsr.cof'
primary output file
   '/scr6/rosen/plt20/plt20c.out'
fixi/fixj output file
   '/scr6/rosen/plt20/plt20c.fix'
wing pressure output file
   '/scr6/rosen/plt20/plt20c.wng'
secondary output file
   '/scr6/rosen/plt20/plt20c.sec'
flowfield output file
   '/scr6/rosen/plt20/plt20c.prt'
unsteady cp output file
   '/scr6/rosen/plt20/plt20c.ucp'
     XMACH     ALPHA      BETA  REUE,MIL   TINF,DR      ISND     C2SPE
     20.00     0.000       0.0  0.200000    100.00         1   10.0000
      SREF      CREF      BREF       XMC       YMC       ZMC
    0.1000    1.0000    0.1000       .05        .5        0.
      IGAS     GAMMA      RGAS     PRGAS    SCALEX    SCALET    SCALEM
         3       1.4     286.9      0.72       1.0       1.0       1.0
        DT     IREST   IFLAGTS      FMAX     IUNST     RFREQ    ALPHAU      CLOC
    -0.001         0      1500   1000.00         0   0.00000   0.00000   0.00000
     NGRID   NPLOT3D    NPRINT    NWREST
         1         0         2       250
       NCG       IEM  IADVANCE    IFORCE     IMESH  IVISC(I)  IVISC(J)  IVISC(K)
         0         0         0         0         0         0         0         1
      IDIM      JDIM      KDIM      ITE1      ITE2      JTE1      JTE2
         2        65        65         1         2         1        65
     INEWG    IGRIDC        IS        JS        KS        IE        JE        KE
         1         0         0         0         0         0         0         0
  IDIAG(I)  IDIAG(J)  IDIAG(K)  IFLIM(I)  IFLIM(J)  IFLIM(K)
         0         0         0         2         2         2
   IFDS(I)   IFDS(J)   IFDS(K)  RKAPO(I)  RKAPO(J)  RKAPO(K)
         1         1         1   0.33333   0.33333   0.33333
 MTYPEI(1) MTYPEI(2) MTYPEJ(1) MTYPEJ(2) MTYPEK(1) MTYPEK(2)
        11        11        27        27        67        67
 NUMBER OF BLOCK INTERFACE BOUNDARY CONDITIONS
   0
 BLOCK INTERFACE BOUNDARY CONDITION ON OR OFF ( >=0 OR <0 )
 BLCK1 IST JST KST IND JND KND IND1 IND2 BLCK2 IST JST KST IND JND KND IND1 IND2
      MSEQ    MGFLAG    ICONSF       MTT      NGAM
         1         0         0         0        01
      NCYC    MGLEVG     NEMGL     NITFO
      1500        01        00       000
      MIT1      MIT2      MIT3      MIT4      MIT5
        01        01        01        01        01
  PRINT OUT:
  BLOCK ISTART    IEND    IINC JSTART    JEND    JINC KSTART    KEND    KINC
      1      2       2       1      64      64       1      1      65       2
      1      2       2       1       2      64       2      1       1       1
```

High Speed Inlet

```
  2-D INLET - AIAA 87-1117 (LIU, VAN LEER)
binary grid file
   '/scr2/rosen/in/in.grd'
binary restart file
   '/scr2/rosen/in/i3.bin'
binary plot3d grid file
   '/scr2/rosen/in/i3.plg'
binary plot3d flowfield file
   '/scr2/rosen/in/i3.plq'
Liu & Vinokur binary equilibrium air coefficient file
   '/scr2/rosen/cfl3dn/liu/liubsr.cof'
primary output file
   '/scr2/rosen/in/i3.out'
fixi/fixj output file
   '/scr2/rosen/in/i3.fix'
wing pressure output file
   '/scr2/rosen/in/i3.wng'
secondary output file
   '/scr2/rosen/in/i3.sec'
flowfield output file
   '/scr2/rosen/in/i3.prt'
unsteady cp output file
   '/scr2/rosen/in/i3.ucp'
     XMACH     ALPHA      BETA  REUE,MIL   TINF,DK      ISND     C2SPE
     5.000     0.000       0.0  4.940578    3573.0         1       1.0
      SREF      CREF      BREF       XMC       YMC       ZMC
       0.1       1.0       0.1       0.5      0.05        0.
      IGAS     GAMMA      RGAS     PRGAS    SCALEX    SCALET    SCALEM
         3       1.4     286.9      0.72       1.0       1.0       1.0
        DT     IREST  IFLAGTS      FMAX     IUNST     RFREQ    ALPHAU      CLOC
    -0.010         0       300     10.00         0   0.00000   0.00000   0.00000
     NGRID   NPLOT3D    NPRINT    NWREST
         1         0         1       100
       NCG       IEM  IADVANCE    IFORCE     IMESH  IVISC(I)  IVISC(J)  IVISC(K)
         0         0         0         0         1         0         0         0
      IDIM      JDIM      KDIM      ITE1      ITE2      JTE1      JTE2
         2       201        51         1         2         1       201
     INEWG    IGRIDC        IS        JS        KS        IE        JE        KE
         1         0         0         0         0         0         0         0
  IDIAG(I)  IDIAG(J)  IDIAG(K)  IFLIM(I)  IFLIM(J)  IFLIM(K)
         0         0         0         2         2         2
   IFDS(I)   IFDS(J)   IFDS(K)  RKAP0(I)  RKAP0(J)  RKAP0(K)
         0         0         0   0.33333   0.33333   0.33333
 MTYPEI(1) MTYPEI(2) MTYPEJ(1) MTYPEJ(2) MTYPEK(1) MTYPEK(2)
        27        27        27        27        27        27
 NUMBER OF BLOCK INTERFACE BOUNDARY CONDITIONS
     0
 BLOCK INTERFACE BOUNDARY CONDITION ON OR OFF ( >=0 OR <0 )
 BLCK1 IST JST KST IND JND KND IND1 IND2 BLCK2 IST JST KST IND JND KND IND1 IND2
      MSEQ    MGFLAG    ICONSF       MTT      NGAM
         1         0         0         0        01
      NCYC    MGLEVG     NEMGL     NITFO
       300        01        00       000
      MIT1      MIT2      MIT3      MIT4      MIT5
        01        01        01        01        01
  PRINT OUT:
  BLOCK ISTART    IEND    IINC JSTART    JEND    JINC KSTART    KEND    KINC
      1      2       2       1      1     201       1      1       1       1
```

Bent Nose Biconic

```
   BENT-BICONIC AT LOW-RE ALPHA=0 (NASA-TP-2334)
binary grid file
   '/scr/rosen/bnb/bnb.grd'
binary restart file
   '/scr/rosen/bnb/b3.bin'
binary plot3d grid file
   '/scr/rosen/bnb/b3.plg'
binary plot3d flowfield file
   '/scr/rosen/bnb/b3.plq'
Liu & Vinokur binary equilibrium air coefficient file
   'liu/liubsr.cof'
primary output file
   '/scr/rosen/bnb/b3.out'
fixi/fixj output file
   '/scr/rosen/bnb/b3.fix'
wing pressure output file
   '/scr/rosen/bnb/b3.wng'
secondary output file
   '/scr/rosen/bnb/b3.sec'
flowfield output file
   '/scr/rosen/bnb/b3.prt'
unsteady cp output file
   '/scr/rosen/bnb/b3.ucp'
     XMACH      ALPHA       BETA  REUE,MIL    TINF,DK       ISND      C2SPE
     9.860      0.000        0.0  1.842000      49.75          1   6.030151
      SREF       CREF       BREF       XMC        YMC        ZMC
  0.001013   0.121680   0.121680  0.067950         0.         0.
      IGAS      GAMMA       RGAS     PRGAS     SCALEX     SCALET     SCALEM
         3        1.4      286.9      0.72        1.0        1.0        1.0
        DT      IREST    IFLAGTS      FMAX      IUNST      RFREQ     ALPHAU       CLOC
    -0.001          0        400     10.00          0    0.00000    0.00000    0.00000
     NGRID    NPLOT3D     NPRINT    NWREST
         1          0          0       100
       NCG        IEM   IADVANCE    IFORCE      IMESH   IVISC(I)   IVISC(J)   IVISC(K)
         1          0          0         0          3          0          0          1
      IDIM       JDIM       KDIM      ITE1       ITE2       JTE1       JTE2
        85         23         45         1         85          1         23
     INEWG     IGRIDC         IS        JS         KS         IE         JE         KE
         1          0          0         0          0          0          0          0
   IDIAG(I)   IDIAG(J)   IDIAG(K)  IFLIM(I)   IFLIM(J)   IFLIM(K)
         0          0          0         2          2          2
    IFDS(I)    IFDS(J)    IFDS(K)  RKAP0(I)   RKAP0(J)   RKAP0(K)
         0          0          0   0.33333    0.33333    0.33333
  MTYPEI(1)  MTYPEI(2)  MTYPEJ(1)  MTYPEJ(2)  MTYPEK(1)  MTYPEK(2)
        33         67          3         3         67         77
  NUMBER OF BLOCK INTERFACE BOUNDARY CONDITIONS
    0
  BLOCK INTERFACE BOUNDARY CONDITION ON OR OFF ( >=0 OR <0 )
  BLCK1 IST JST KST IND JND KND IND1 IND2 BLCK2 IST JST KST IND JND KND IND1 IND2
      MSEQ     MGFLAG     ICONSF       MTT       NGAM
         2          0          0         0         01
      NCYC     MGLEVG      NEMGL     NITFO
       400         01         00       000
       000         01         00       000
      MIT1       MIT2       MIT3      MIT4       MIT5
        01         01         01        01         01
        01         01         01        01         01
   PRINT OUT:
   BLOCK ISTART      IEND     IINC JSTART      JEND      JINC KSTART     KEND      KINC
       1      1        85        1      1        23         1      1        1         1
```

Flared Cone (Laminar)

```
  A50-FLARED-CONE AT LOW-RE RUN-17 (AFFDL-TR-65-199)
binary grid file
   '/scr2/rosen/a50/a50.grd'
binary restart file
   '/scr2/rosen/a50/a3.bin'
binary plot3d grid file
   '/scr2/rosen/a50/a3.plg'
binary plot3d flowfield file
   '/scr2/rosen/a50/a3.plq'
Liu & Vinokur binary equilibrium air coefficient file
   '/scr2/rosen/cfl3dn/liu/liubsr.cof'
primary output file
   '/scr2/rosen/a50/a3.out'
fixi/fixj output file
   '/scr2/rosen/a50/a3.fix'
wing pressure output file
   '/scr2/rosen/a50/a3.wng'
secondary output file
   '/scr2/rosen/a50/a3.sec'
flowfield output file
   '/scr2/rosen/a50/a3.prt'
unsteady cp output file
   '/scr2/rosen/a50/a3.ucp'
     XMACH      ALPHA       BETA  REUE,MIL    TINF,DR       ISND      C2SPE
    16.930      0.000        0.0  0.197600      83.73          1   6.329870
      SREF       CREF       BREF       XMC        YMC        ZMC
       1.0        1.0        1.0       1.0         0.         0.
      IGAS      GAMMA       RGAS     PRGAS     SCALEX     SCALET     SCALEM
         3        1.4     1715.6      0.72        0.0        0.0        0.0
        DT      IREST    IFLAGTS      FMAX      IUNST      RFREQ     ALPHAU       CLOC
    -0.001          0        300     10.00          0    0.00000    0.00000    0.00000
     NGRID    NPLOT3D     NPRINT    NWREST
         1          0          0       100
       NCG        IEM   IADVANCE    IFORCE      IMESH   IVISC(I)   IVISC(J)   IVISC(K)
         1          0          0         0          1          0          0          1
      IDIM       JDIM       KDIM      ITE1       ITE2       JTE1       JTE2
        97         19         45         5         97          1         19
     INEWG     IGRIDC         IS        JS         KS         IE         JE         KE
         1          0          0         0          0          0          0          0
  IDIAG(I)   IDIAG(J)   IDIAG(K)  IFLIM(I)   IFLIM(J)   IFLIM(K)
         0          0          0         2          2          2
   IFDS(I)    IFDS(J)    IFDS(K)  RKAP0(I)   RKAP0(J)   RKAP0(K)
         1          1          1   0.33333    0.33333    0.33333
 MTYPEI(1) MTYPEI(2) MTYPEJ(1) MTYPEJ(2) MTYPEK(1) MTYPEK(2)
        67         67         1         1         67         77
 NUMBER OF BLOCK INTERFACE BOUNDARY CONDITIONS
   0
 BLOCK INTERFACE BOUNDARY CONDITION ON OR OFF ( >=0 OR <0 )
 BLCK1 IST JST KST IND JND KND IND1 IND2 BLCK2 IST JST KST IND JND KND IND1 IND2
      MSEQ     MGFLAG     ICONSF       MTT       NGAM
         2          0          0         0         01
      NCYC     MGLEVG      NEMGL     NITFO
       300         01         00       000
       000         01         00       000
      MIT1       MIT2       MIT3      MIT4       MIT5
        01         01         01        01         01
        01         01         01        01         01
  PRINT OUT:
  BLOCK ISTART    IEND    IINC JSTART    JEND    JINC KSTART    KEND    KINC
      1      1      97       1      1      19       1      1       1       1
```

Flared Cone (Turbulent)

```
  A50-FLARED-CONE AT HIGH-RE RUN-32 (AFFDL-TR-65-199)
binary grid file
   '/scr/rosen/a32/a32.grd'
binary restart file
   '/scr/rosen/a32/a3.bin'
binary plot3d grid file
   '/scr/rosen/a32/a3.plg'
binary plot3d flowfield file
   '/scr/rosen/a32/a3.plq'
Liu & Vinokur binary equilibrium air coefficient file
   'liu/liubsr.cof'
primary output file
   '/scr/rosen/a32/a3.out'
fixi/fixj output file
   '/scr/rosen/a32/a3.fix'
wing pressure output file
   '/scr/rosen/a32/a3.wng'
secondary output file
   '/scr/rosen/a32/a3.sec'
flowfield output file
   '/scr/rosen/a32/a3.prt'
unsteady cp output file
   '/scr/rosen/a32/a3.ucp'
     XMACH      ALPHA       BETA  REUE,MIL   TINF,DR       ISND      C2SPE
     7.850      0.000        0.0  4.697000     130.2          1   4.070661
      SREF       CREF       BREF       XMC       YMC        ZMC
       1.0        1.0        1.0       1.0        0.         0.
      IGAS      GAMMA       RGAS     PRGAS    SCALEX     SCALET     SCALEM
         3        1.4     1715.6      0.72       0.0        0.0        0.0
        DT      IREST   IFLAGTS       FMAX     IUNST      RFREQ     ALPHAU       CLOC
    -0.010          0        300     10.00         0    0.00000    0.00000    0.00000
     NGRID    NPLOT3D     NPRINT    NWREST
         2          0          0       100
       NCG        IEM   IADVANCE    IFORCE     IMESH   IVISC(I)   IVISC(J)   IVISC(K)
         1          0          0         0         1          0          0          0
         1          0          0         0         1          0          0          1
      IDIM       JDIM       KDIM      ITE1      ITE2       JTE1       JTE2
         5         19         45         5         5          1         19
        93         19         45         1        93          1         19
     INEWG     IGRIDC         IS        JS        KS         IE         JE         KE
         1          0          0         0         0          0          0          0
         1          0          0         0         0          0          0          0
  IDIAG(I)   IDIAG(J)   IDIAG(K)  IFLIM(I)  IFLIM(J)   IFLIM(K)
         0          0          0         2         2          2
         0          0          0         2         2          2
   IFDS(I)    IFDS(J)    IFDS(K)  RKAP0(I)  RKAP0(J)   RKAP0(K)
         1          1          1   0.33333   0.33333    0.33333
         1          1          1   0.33333   0.33333    0.33333
 MTYPEI(1) MTYPEI(2) MTYPEJ(1) MTYPEJ(2) MTYPEK(1) MTYPEK(2)
        67         67          1         1        67         77
        67         67          1         1        67         77
 NUMBER OF BLOCK INTERFACE BOUNDARY CONDITIONS
    1
 BLOCK INTERFACE BOUNDARY CONDITION ON OR OFF ( >=0 OR <0 )
    1
 BLCK1 IST JST KST IND JND KND IND1 IND2 BLCK2 IST JST KST IND JND KND IND1 IND2
     1   5   1   1   5  19  45    2    3     2   1   1   1   1  19  45    2    3
      MSEQ     MGFLAG     ICONSF       MTT      NGAM
         2          0          0         0        01
      NCYC     MGLEVG      NEMGL     NITFO
       300         01         00       000
       000         01         00       000
      MIT1       MIT2       MIT3      MIT4      MIT5
        01         01         01        01        01
        01         01         01        01        01
```

Laminar Corner Flow

```
   symmetric wedge corner : liu,lam
binary grid file
   '/scr2/rosen/corner/lam.grd'
binary restart file
   '/scr2/rosen/corner/l3.bin'
plot3d binary grid file
   '/scr2/rosen/corner/l3.plg'
plot3d binary flowfield file
   '/scr2/rosen/corner/l3.plq'
Liu & Vinokur binary equilibrium air coefficient file
   'liu/liubsr.cof'
primary output file
   '/scr2/rosen/corner/l3.out'
fixi/fixj output file
   '/scr2/rosen/corner/l3.fix'
wing pressure output file
   '/scr2/rosen/corner/l3.wng'
secondary output file
   '/scr2/rosen/corner/l3.sec'
flowfield output file
   '/scr2/rosen/corner/l3.prt'
unsteady cp output file
   '/scr2/rosen/corner/l3.ucp'
     XMACH     ALPHA      BETA  REUE,MIL   TINF,DK      ISND     C2SPE
      3.00     0.000       0.0      3.07     105.0         1       2.8
      SREF      CREF      BREF       XMC       YMC       ZMC
    1.0000    1.0000    1.0000       0.0       0.0       0.0
      IGAS     GAMMA      RGAS     PRGAS    SCALEX    SCALET    SCALEM
         3       1.4     286.9      0.72       1.0       1.0       1.0
        DT     IREST   IFLAGTS      FMAX     IUNST     RFREQ    ALPHAU      CLOC
    -0.010         0       300     10.00         0   0.00000   0.00000   0.00000
     NGRID   NPLOT3D    NPRINT    NWREST
         1         0         0       300
       NCG       IEM  IADVANCE    IFORCE     IMESH  IVISC(I)  IVISC(J)  IVISC(K)
         0         0         0         0         0         0         1         1
      IDIM      JDIM      KDIM      ITE1      ITE2      JTE1      JTE2
         2       121       121         1         2         1       121
     INEWG    IGRIDC        IS        JS        KS        IE        JE        KE
         1         0         0         0         0         0         0         0
  IDIAG(I)  IDIAG(J)  IDIAG(K)  IFLIM(I)  IFLIM(J)  IFLIM(K)
         0         0         0         2         2         2
   IFDS(I)   IFDS(J)   IFDS(K)  RKAP0(I)  RKAP0(J)  RKAP0(K)
         1         1         1   0.33333   0.33333   0.33333
 MTYPEI(1) MTYPEI(2) MTYPEJ(1) MTYPEJ(2) MTYPEK(1) MTYPEK(2)
      1002      1002      1004      1002      1004      1002
 NUMBER OF BLOCK INTERFACE BOUNDARY CONDITIONS
     0
 BLOCK INTERFACE BOUNDARY CONDITION ON OR OFF ( >=0 OR <0 )
 BLCK1 IST JST KST IND JND KND IND1 IND2 BLCK2 IST JST KST IND JND KND IND1 IND2
      MSEQ    MGFLAG    ICONSF       MTT      NGAM
         1         0         0         0        01
      NCYC    MGLEVG     NEMGL     NITFO
       300        01        00       000
      MIT1      MIT2      MIT3      MIT4      MIT5
        01        01        01        01        01
```

Turbulent Corner Flow

```
   symmetric wedge corner : liu,turbulent
binary grid file
   '/scr2/rosen/corner/turb3.grd'
binary restart file
   '/scr2/rosen/corner/t3.bin'
plot3d binary grid file
   '/scr2/rosen/corner/t3.plg'
plot3d binary flowfield file
   '/scr2/rosen/corner/t3.plq'
Liu & Vinokur binary equilibrium air coefficient file
   'liu/liubsr.cof'
primary output file
   '/scr2/rosen/corner/t3.out'
fixi/fixj output file
   '/scr2/rosen/corner/t3.fix'
wing pressure output file
   '/scr2/rosen/corner/t3.wng'
secondary output file
   '/scr2/rosen/corner/t3.sec'
flowfield output file
   '/scr2/rosen/corner/t3.prt'
unsteady cp output file
   '/scr2/rosen/corner/t3.ucp'
     XMACH      ALPHA       BETA   REUE,MIL    TINF,DK       ISND      C2SPE
      3.00      0.000        0.0     3.2189      105.0          1        2.8
      SREF       CREF       BREF        XMC        YMC        ZMC
    1.0000     1.0000     1.0000        0.0        0.0        0.0
      IGAS      GAMMA       RGAS      PRGAS     SCALEX     SCALET     SCALEM
         3        1.4      286.9       0.72        1.0        1.0        1.0
        DT      IREST    IFLAGTS       FMAX      IUNST      RFREQ     ALPHAU       CLOC
    -0.010          0        300      10.00          0    0.00000    0.00000    0.00000
     NGRID    NPLOT3D     NPRINT    NWREST
         1          0          0        300
       NCG        IEM   IADVANCE     IFORCE      IMESH   IVISC(I)   IVISC(J)   IVISC(K)
         0          0          0          0          0          0          1          1
      IDIM       JDIM       KDIM       ITE1       ITE2       JTE1       JTE2
         2        121        121          1          2          1        121
     INEWG     IGRIDC         IS         JS         KS         IE         JE         KE
         1          0          0          0          0          0          0          0
  IDIAG(I)   IDIAG(J)   IDIAG(K)   IFLIM(I)   IFLIM(J)   IFLIM(K)
         0          0          0          2          2          2
   IFDS(I)    IFDS(J)    IFDS(K)   RKAP0(I)   RKAP0(J)   RKAP0(K)
         1          1          1    0.33333    0.33333    0.33333
MTYPEI(1) MTYPEI(2) MTYPEJ(1) MTYPEJ(2) MTYPEK(1) MTYPEK(2)
      1002       1002       1004       1002       1004       1002
NUMBER OF BLOCK INTERFACE BOUNDARY CONDITIONS
  0
BLOCK INTERFACE BOUNDARY CONDITION ON OR OFF ( >=0 OR <0 )
BLCK1 IST JST KST IND JND KND IND1 IND2 BLCK2 IST JST KST IND JND KND IND1 IND2
      MSEQ     MGFLAG     ICONSF        MTT       NGAM
         1          0          0          0         01
      NCYC     MGLEVG      NEMGL     NITFO
       300         01         00        000
      MIT1       MIT2       MIT3       MIT4       MIT5
        01         01         01         01         01
```

Report Documentation Page

NASA National Aeronautics and Space Administration

1. Report No.	NASA TM-102616
2. Government Accession No.	
3. Recipient's Catalog No.	
4. Title and Subtitle	Addition of Equilibrium Air to an Upwind Navier-Stokes Code and Other First Steps Toward A More Generalized Flow Solver
5. Report Date	March 1991
6. Performing Organization Code	
7. Author(s)	Bruce S. Rosen
8. Performing Organization Report No.	
9. Performing Organization Name and Address	NASA Langley Research Center Hampton, VA 23665-5225
10. Work Unit No.	505-80-11-02
11. Contract or Grant No.	
12. Sponsoring Agency Name and Address	National Aeronautics and Space Administration Washington, DC 20546-0001
13. Type of Report and Period Covered	Technical Memorandum
14. Sponsoring Agency Code	

15. Supplementary Notes

The work described herein was completed under a Memorandum of Understanding between the NASA Langley Research Center and Grumman Aircraft Systems Division dated July 1988.

Bruce S. Rosen: Grumman Aircraft Systems Division, Bethpage, New York 11714

16. Abstract

An upwind 3-D finite volume Navier-Stokes code is modified to facilitate modeling of complex geometries and flow fields presented by proposed National Aero-Space Plane concepts. Code enhancements include an equilibrium air model, a generalized equilibrium gas model, and several schemes to simplify treatment of complex geometric configurations. The code is also restructured for inclusion of an arbitrary number of independent and dependent variables. This latter capability is intended for eventual use to incorporate nonequilibrium/chemistry gas models, more sophisticated turbulence and transition models, and other physical phenomena which will require inclusion of additional variables and/or governing equations. Comparisons of computed results with experimental data and with results obtained using the other methods are presented for code validation purposes. Good correlation is obtained for all of the test cases considered, indicating the success of the current effort. This work was conducted at the NASA Langley Research Center, during participation in the NASA/Industry Fellowship Program for the National Aero-Space Plane.

17. Key Words (Suggested by Author(s))	18. Distribution Statement
Hypersonics National Aero-Space Plane Program Computational Fluid Dynamics Real Gas	Unclassified-Unlimited Subject Category 34

19. Security Classif. (of this report)	20. Security Classif. (of this page)	21. No. of pages	22. Price
Unclassified	Unclassified	50	A03